REVIEW ARTICLE

Empowering Breast Cancer Precision Diagnosis with Advanced Ultrasound: From Radiomics to Radio-multiomics

***Mo Li*[a,b,c], *Letian Jin*[a,b,c], *Ge Xue*[d], *Jiye Chen*[b,c], *Mohamed Aimene Benariba*[e], *Vicky Yang Wang*[b,f,g], *Gaojun Teng*[c,e,h], *Dong Xu*[a,b,c,e,f,g,*]**

[a] *Wenzhou Medical University, Wenzhou, Zhejiang, China;* [b] *Department of Diagnostic Ultrasound Imaging & Interventional Therapy, Zhejiang Cancer Hospital, Hangzhou Institute of Medicine (HIM), Chinese Academy of Sciences, Hangzhou, Zhejiang, China;* [c] *Center of Interventional Oncology, Zhejiang Cancer Hospital, Hangzhou Institute of Medicine (HIM), Chinese Academy of Sciences, Hangzhou, Zhejiang, China;* [d] *The Quzhou Affiliated Hospital of Wenzhou Medical University (Quzhou People's Hospital), Quzhou, China;* [e] *Research Center of Interventional Medicine and Engineering, Hangzhou Institute of Medicine (HIM), Chinese Academy of Sciences, Hangzhou, Zhejiang, China;* [f] *Center of Intelligent Diagnosis and Therapy (Taizhou), Zhejiang Cancer Hospital, Hangzhou Institute of Medicine (HIM), Chinese Academy of Sciences, Hangzhou, Zhejiang, China;* [g] *Wenling Institute of Big Data and Artificial Intelligence in Medicine, Taizhou, Zhejiang, China;* [h] *Center of Interventional Radiology and Vascular Surgery, Nurturing Center of Jiangsu Province for State Laboratory of AI Imaging & Interventional Radiology (Southeast University), Department of Radiology, Zhongda Hospital, Medical School, Southeast University, Nanjing, Jiangsu, China*

Received September 18, 2026; revision requested October 17, 2026; accepted November 21, 2026

Abstract: Numerous research studies have revealed that breast cancer is characterized by substantial biological and molecular heterogeneity, which can neither be fully captured by conventional clinical medical imaging nor biopsy which is typically limited by sampling error and invasiveness. Despite the exhibited complexity, developments in ultrasound imaging technologies from morphological imaging only to multi-dimensional functional imaging coupled with quantitative analysis have significantly improved the diagnostic accessibility and efficiency for breast cancer patients. This review first summarizes recent advances in multi-modal ultrasound imaging encompassing microvascular and super-resolution ultrasound imaging with contrast enhancement, elastography and viscoelastic imaging, as well as quantitative analysis consisting of radiofrequency signal analysis, radiomics, and artificial intelligence-based image analysis for precision breast cancer diagnosis. Specific attention is given to their applications in benign-malignant differentiation, molecular subtype characterization, lymph node metastasis assessment. Beyond image-based analysis, the integration of ultrasound radiomics with genomic, transcriptomic, and other multi-omics data is emerging as a promising strategy for non-invasive molecular phenotyping, although its clinical application is still at its infancy. This review then discusses the transition from radiomics alone through radiogenomics to radio-multiomics, highlighting the potential of advanced ultrasound imaging technologies to bridge imaging phenotypes with underlying tumor biological behaviour in order to facilitate individualized diagnosis and treatment planning. Most radio-multiomics approaches remain at a preclinical or proof-of-concept stage and still require validation in large-scale paired cohorts. In addition, issues such as standardization, reproducibility, interpretability and data heterogeneity remain to be resolved. Finally, this review discusses current challenges that should be addressed before ultrasound-based radio-multi-omics can be translated to a viable clinical tool.

Key words: Breast cancer; Advanced ultrasound; Ultrasound radiomics; Artificial intelligence; Radio-multiomics; Precision diagnosis

Advanced Ultrasound in Diagnosis and Therapy 2026; 04: 277-297 DOI: 10.26599/AUDT.2026.260041

[*] *Corresponding author: Zhejiang Cancer Hospital, No. 1 Banshan East Road, Gongshu District, Hangzhou, Zhejiang 310022, China (Dong Xu)*
e-mail: xudong@zjcc.org.cn (D X)

2576-2508/© AUDT 2026 • http://www.AUDT.org
This is an open-access article distributed under the terms of the Creative Commons Attribution 4.0 International license, which permits unrestricted use, distribution and reproduction in any medium provided that the original work is properly attributed.

Breast cancer is the most commonly diagnosed malignancy among women worldwide and the second leading cause of cancer-related mortality in women [1,2] with the first leading cause being lung cancer in many countries. In 2022, approximately 2.3 million new cases of breast cancer and 670, 000 breast cancer-related deaths were reported among women worldwide [2]. The clinical diagnostic paradigm for breast cancer has undergone a fundamental shift, from traditional macroscopic anatomical staging toward precision risk stratification based on molecular subtypes, including estrogen receptor (ER), progesterone receptor (PR), human epidermal growth factor receptor 2 (HER2), and Ki-67 [3] which are the key factors influencing treatment planning. However, the high spatiotemporal heterogeneity of breast cancer poses substantial challenges to precision diagnosis [4]. On one hand, the determination of molecular subtypes relies heavily on invasive biopsy and/or pathological examination, and such localized sampling may fail to comprehensively capture the three-dimensional spatial characteristics of the tumor in addition to the invasiveness which also limits dynamic tracking of disease progression. On the other hand, current breast imaging primarily relies on macroscopic morphological features for lesion assessment, leaving a persistent information gap between imaging phenotypes and the tumor's microscopic molecular and biological characteristics.

Currently, mammography remains an important imaging modality for breast cancer screening and early diagnosis, offering strong capability for detecting microcalcifications with a high degree of standardization; however, its diagnostic performance can be affected by breast density [5,6] which have proven to be less preferred for Asian women. Magnetic resonance imaging (MRI) provides high sensitivity and excellent soft-tissue contrast, and plays an important role in screening high-risk populations, assessing the extent of lesions, and preoperative staging. Nevertheless, its relatively high cost and limited accessibility, together with its suboptimal specificity, constrain its broader clinical application [6]. Therefore, although mammography and MRI each offer distinct advantages in breast cancer screening and diagnosis, both imaging modalities remain limited in their ability to noninvasively characterize tumor microvasculature, tissue mechanical properties, and microscopic biological features.

In comparison, ultrasound (US) imaging has become an important imaging modality for breast assessment owing to its portability, radiation-free, real-time, and efficient characteristics [7]. In recent years, advanced US technologies have made substantial progress in both image acquisition and analysis, offering new opportunities to overcome the limitations of conventional approaches to affordable and precision diagnosis. At the image acquisition level, emerging US techniques have evolved beyond conventional anatomical imaging toward multi-modal functional characterization of the tumor microvascular network and the biomechanical properties of the tumor. At the image analysis level, the integration of quantitative US techniques with artificial intelligence (AI) algorithms has enabled the extraction of subtle, otherwise imperceptible features from conventional images, allowing further exploitation of the abundant imaging information. The development of radiomics also enabled transformation of complex imaging information into high-throughput quantitative data, providing a quantitative framework for the objective assessment of breast cancer.

Furthermore, imaging phenotypes alone remain insufficient to fully capture the complex biological heterogeneity of breast cancer. Integrating ultrasound imaging features with multi-omics molecular data, such as genomic and transcriptomic profiles, may help establish associations between imaging phenotypes and tumor molecular characteristics, thereby further elucidating the underlying biological mechanisms and enabling precision diagnosis at a higher dimensional level [8].

To this end, this review systematically summarizes the development of emerging US technologies for precision diagnosis of breast cancer, with particular focuses on progress in multi-modal functional US image acquisition and AI-driven image analysis, followed by an evaluation of their clinical diagnostic performance and limitations, and lastly an outlook of the emerging trend toward US-based multi-omics approach. This review is structured as follows: advances in imaging technologies, ranging from structural imaging through microvascular imaging to modality for assessing mechanical properties are presented in Section 2; analysis strategies for ultrasound imaging data, ranging from manual quantification to AI-enabled approaches are summarized in Section 3; the latest progression in the application of ultrasound imaging to breast cancer screening and diagnosis are discussed in Section 4; and finally a prospective discussion on the ongoing research spanning from single-omics feature mining to multi-omics mechanistic integration aiming to provide a solid theoretical foundation for exploring precise diagnosis of breast cancer, is shown in Section 5. A succinct summary of the key techniques and methodologies discussed in this review is illustrated in figure 1.

The literature reviewed in this article was identified through keyword searches in PubMed, supplemented by Google Scholar. Search terms combined "breast cancer"

清華大學出版社 Tsinghua University Press | SciOpen

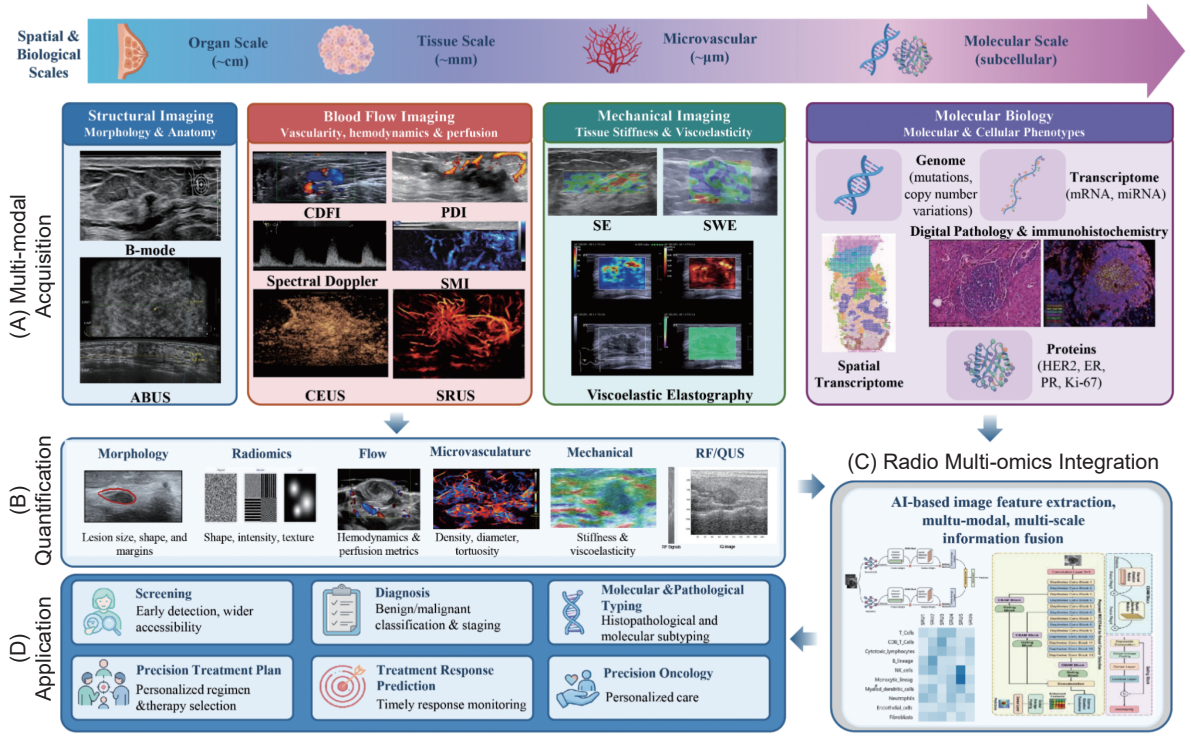


Figure 1 From multi-modal ultrasound acquisition to radio-multiomics in breast cancer. Four stages are linked across the organ (~cm), tissue (~mm), microvascular (~μm), and molecular (subcellular) scales. (A) Multi-modal acquisition covers structural imaging (B-mode, ABUS), blood flow imaging (CDFI, PDI, spectral Doppler, SMI, CEUS, SRUS), mechanical imaging (SE, SWE, viscoelastic elastography), and molecular biology (genome, transcriptome, digital pathology and IHC, spatial transcriptome, proteins); (B) Quantification yields morphological and radiomic features, hemodynamic and perfusion metrics, microvascular density, diameter and tortuosity, stiffness and viscoelasticity, and RF/QUS parameters; (C) AI extracts and fuses multi-modal, multi-scale image features that link imaging phenotypes to molecular subtypes and immune cell infiltration; (D) The model serves six clinical applications: screening, diagnosis, molecular and pathological typing, precision treatment planning, treatment response prediction, and personalized care. Abbreviations: ABUS, automated breast ultrasound; AI, artificial intelligence; B-mode, grayscale ultrasound; CDFI, color Doppler flow imaging; CEUS, contrast-enhanced ultrasound; ER, estrogen receptor; HER2, human epidermal growth factor receptor 2; IHC, immunohistochemistry; miRNA, microRNA; mRNA, messenger RNA; PDI, power Doppler imaging; PR, progesterone receptor; QUS, quantitative ultrasound; RF, radiofrequency; SE, strain elastography; SMI, superb microvascular imaging; SRUS, super-resolution ultrasound; SWE, shear wave elastography.

with terms related to the ultrasound techniques and analysis approaches discussed in this review, including contrast-enhanced ultrasound, super-resolution ultrasound and microvascular imaging, elastography and viscoelasticity, radiomics, artificial intelligence, and multi-omics. The search covered publications available up to September 2026, with an emphasis on studies published within the preceding five years. Eligible publications included peer-reviewed original research articles, relevant reviews, and society guidelines and addressing ultrasound-based imaging or quantification approaches relevant to breast cancer. Conference abstracts, preprints, non-English publications, and studies with limited relevance to the scope of this review were excluded. Seminal earlier studies were also considered where relevant.

Advancements in Ultrasound Techniques

Structural imaging

Since the 1950s, breast ultrasound technology had been developed based on the pulse-echo principle and differences in acoustic impedance between tissues. Its imaging paradigm has undergone a fundamental transition from one-dimensional waveforms that record the amplitude of echoes reflected from tissue interfaces, known as amplitude mode (A-mode), to two-dimensional anatomical imaging in which echo amplitudes are mapped to grayscale values to reconstruct images, known as brightness mode (B-mode).

Currently, B-mode ultrasound has become the primary imaging modality for clinical breast examination and risk assessment. In particular, it provides a unique clinical benefit in compensating for the limited detection of lesions in dense breasts by mammography [9,10]. At present, the clinical interpretation of two-dimensional ultrasound images primarily relies on the Breast Imaging Reporting and Data System (BI-RADS), which uses standardized terminology to characterize lesion features, including morphology, margins, internal echogenicity, and orientation, thereby providing an objective basis for risk stratification of benign and malignant lesions [11]. Meanwhile, the spatial information provided by B-mode ultrasound serves as an anatomical reference for multimodal US techniques, including color Doppler, elastog-

raphy, and contrast-enhanced ultrasound (CEUS).

The quality of B-mode image acquisition directly affects the reliability of image interpretation, hence the completeness and accuracy of diagnostic information. Therefore, standardized image acquisition is a prerequisite for ensuring imaging reproducibility and enabling subsequent multimodal analysis. A standardized scanning approach requires operators to systematically acquire and retain transverse, longitudinal, and maximal long-axis images of the target lesion, while also ensuring sufficient documentation of representative or characteristic sonographic findings from static images [10]. Building on this, dynamic video acquisition can further preserve the three-dimensional morphology and spatial relationships of lesions via continuous scanning, providing richer diagnostic information than single-frame static images [10].

(Micro)Vasculature imaging

Doppler Ultrasound Ultrasound Doppler techniques are based on the Doppler effect to obtain blood flow information by detecting frequency shifts generated by moving red blood cells. Commonly used clinical modalities include color Doppler flow imaging (CDFI), power Doppler imaging (PDI), and spectral Doppler (SD), which are primarily used to characterize the direction and velocity of blood flow, the intensity of blood flow signals and low-velocity flow, and local hemodynamic parameters, respectively. Among these modalities, CDFI and PDI are mainly used for blood flow visualization, whereas SD enables further quantitative analysis of parameters such as blood flow velocity and the resistance index.

In clinical practice, color Doppler flow imaging (CDFI) is the most commonly used modality for evaluating tumor angiogenesis in breast ultrasound, enabling direct and dynamic visualization of blood flow velocity and the spatial distribution of vessels within breast masses. Studies have shown that malignant breast tumors typically exhibit abundant blood flow signals on CDFI, with vessels predominantly distributed centrally and displaying a tortuous course. These vascular features are closely associated with abnormal angiogenesis, which plays a key role in the invasive growth of tumors [12]. During routine examination, the combination of CDFI and B-mode ultrasound can significantly improve diagnostic accuracy as shown by an earlier multicenter study involving 1,351 breast masses demonstrating that their combination increased diagnostic specificity from 61.5% to 69.2% ($P < 0.0001$) [13]. However, its sensitivity for detecting microvessels smaller than 0.1 mm is limited, making it difficult to distinguish small or hypovascular breast cancers from hypervascular benign tumors [14]. Beyond conventional differentiation between benign and malignant lesions, CDFI also shows potential value for the noninvasive prediction of molecular subtypes of breast cancer. Zhu et al. investigated the association between CDFI blood flow signals and molecular subtypes of breast cancer. Multivariate logistic regression analysis revealed that the degree of vascularity was significantly associated with specific molecular subtypes, and CDFI findings could serve as independent predictors of Luminal A subtype, which tended to exhibit hypovascularity ($P = 0.036$, OR = 1.107), and triple-negative breast cancer (TNBC), which tended to exhibit hypervascularity ($P = 0.002$, odds ratio [OR] = 0.106), suggesting its potential as an imaging biomarker for molecular subtype assessment [15]. Furthermore, Li et al. combined CDFI with peripheral blood microRNAs (miR-21 and miR-27a). The combined detection approach achieved significantly higher sensitivity (94.57%), accuracy (88.27%), and negative predictive value (83.72%) than either single-marker detection or pairwise combinations ($P < 0.05$), confirming the high complementarity between macroscopic blood flow features and microscopic molecular biomarkers in providing diagnostic information [16].

At the quantitative level, spectral Doppler ultrasound has been investigated for differentiating benign and malignant breast masses using the resistance index (RI), pulsatility index (PI), and peak systolic velocity (PSV). Mehdikhani et al. [17] and Keshavarz et al. [18] reported significantly higher RI, PI, and PSV values in malignant masses, with PI showing the best diagnostic performance (AUCs of 0.882 and 0.90, respectively). However, these parameters are not routinely used as standalone diagnostic criteria, and their reported cutoff values vary across studies.

Contrast-enhanced Ultrasound CEUS is a pure blood-pool microvascular imaging technique often performed after B-mode ultrasound to capture the microcirculatory status of the target region by intravenously or locally administering ultrasound contrast agent and tracking its distribution in real time. CEUS exploits the non-linear oscillation characteristics of contrast agent (i.e. microbubbles) under a low-mechanical-index ultrasound field. By selectively extracting microbubble harmonic signals to suppress background tissue signals, CEUS substantially improves the signal-to-noise ratio of microvascular blood flow.

The most commonly used contrast agents for breast CEUS are Sonazoid® and SonoVue®. Taking the more widely used SonoVue® as an example, compared with Sonazoid®, it has a shorter intranodal retention time during sentinel lymph node (SLN) imaging in the breast. Although this characteristic may be less advantageous

清華大學出版社 Tsinghua University Press | SciOpen

when prolonged intraoperative guidance is required, it can effectively shorten the examination workflow in routine preoperative localization, particularly in clinical studies requiring multiple injections or repeated examinations [19].

In differential diagnosis, malignant breast masses typically exhibit characteristic CEUS features, including hyperenhancement, rapid and early enhancement, centripetal perfusion, penetrating vessels, and perfusion defects [20,21]. These features can aid the differentiation of benign and malignant lesions and may help refine risk stratification of BI-RADS 3-4 lesions, potentially reducing unnecessary biopsy. However, the interpretation of these morphological features is highly dependent on the subjective experience of radiologists. To address this issue, Chen et al. proposed a CEUS-based spatiotemporal analysis method that quantified intralesional enhancement heterogeneity by calculating the similarity of time-intensity curves (TICs) between adjacent pixels using four parameters, including the correlation coefficient (r), spectral coherence (ρ), mutual information (I), and conditional entropy (H). This method enables automated quantitative assessment of CEUS enhancement heterogeneity and may help reduce interobserver variability in subjective interpretation. However, it is currently applicable only to lesions with sufficient enhancement, and future studies should further incorporate three-dimensional imaging or multiparametric ultrasound to expand its applicability [22].

CEUS also demonstrates unique advantages in the evaluation of specific types of breast lesions. Wang et al. investigated the CEUS features of ductal abnormalities and found that microcalcifications (OR = 8.96, P = 0.047) and an enlarged enhancement range (OR = 27.42, P = 0.018) were independent risk factors for predicting malignant ductal lesions. The combination of these two features achieved an area under the curve (AUC) of 0.92, with a sensitivity of 89.5% and a specificity of 88.6%, significantly outperforming either feature alone [23]. For lesions confirmed as atypical ductal hyperplasia (ADH) by core needle biopsy, Li et al. investigated the value of CEUS in predicting postoperative malignant upgrade. Compared with conventional ultrasound, CEUS-adjusted BI-RADS classification, using category 4B as the threshold, significantly improved the sensitivity for predicting malignant upgrade (96.2% vs. 79.2%, P = 0.012) and negative predictive value (95.0% vs. 79.2%, P = 0.030), effectively reducing the risk of missed malignancy. Subgroup analysis further indicated that, for small ADH lesions with a maximum diameter of ≤ 2 cm, the specificity of CEUS-adjusted BI-RADS classification was significantly higher than that of conventional ultrasound (76.7% vs. 13.7%, P = 0.012) [24].

Microflow Imaging In contrast to CEUS, microvascular flow imaging techniques, such as Superb Microvascular Imaging (SMI) and Microvascular Flow Imaging (MVFI), are noninvasive microvascular imaging techniques that do not require intravenous administration of contrast agents. These techniques employ novel adaptive algorithms, including advanced noise reduction, motion artifact suppression, and adaptive filtering, to distinguish true blood flow signals from tissue motion artifacts, thereby enabling the detection of low-velocity blood flow in small vessels that would otherwise be obscured by clutter. Compared with conventional Doppler techniques, SMI significantly improves the sensitivity for detecting microvascular blood flow, as demonstrated by multiple studies [25,26].

Regarding imaging parameters, studies of breast SMI have primarily used high-frequency linear-array transducers with frequencies of approximately 7-18 MHz [27,28] or L14-5 MHz [29-31]. Some studies have also used linear-array transducers with a frequency range of 2-14 MHz [26]. SMI was consistently performed using low-velocity scale settings to optimize microvascular visualization, although the specific velocity ranges varied slightly across studies, including 1.0-2.0 cm/s [29], 1.2-1.6 cm/s [31], 2.5 cm/s [27] and 1.0-1.5 cm/s [26]. The frame rate was generally set at 13-59 frames/s [27,29,31,32], while the pulse repetition frequency (PRF) was mostly in the range of 15.4-20.2 kHz [29,31]. These variations in imaging parameters may contribute to heterogeneity in quantitative SMI measurements and bias in vascular architecture classification, highlighting the need to prioritize standardization of SMI parameter settings in clinical implementation.

Super-resolution US Super-resolution ultrasound (SRUS), also known as ultrasound localization microscopy (ULM), is an emerging *in vivo* imaging technique for visualizing microvasculature in deep tissues. By repeatedly localizing and tracking individual contrast microbubbles across consecutive image frames, this technique reconstructs vascular structures at sub-diffraction resolution, thereby achieving spatial resolution beyond the conventional limits of ultrasound imaging [33,34]. According to the Abbe diffraction limit, the spatial resolution of conventional ultrasound is limited by the acoustic wavelength, approximately λ/2. SRUS overcomes this limitation through precise localization of microbubble centers, with some studies achieving a resolution of λ/10 or better, approximately fivefold beyond the diffraction limit. In absolute terms, the spatial resolution achieved in preclinical and clinical imaging can reach 25 μm [33], The highest spatial resolution can even reach 10-μm range [35], representing an approximately one-order-of-magnitude improvement over con-

ventional ultrasound. However, because microbubble localization requires the acquisition of a massive number of image frames, the prolonged scanning time has become a major bottleneck limiting its clinical translation [33]. To address this issue, Opacic et al. proposed motion-model ultrasound localization microscopy (mULM), which incorporates a Markov chain Monte Carlo data association (MCMCDA) algorithm to achieve robust microbubble tracking at a conventional ultrasound frame rate of approximately 50 frames/s, reduced the effective scanning time to 40 s in that study, which may improve clinical feasibility [36].

In studies of breast SRUS, hardware selection has generally favored high-frequency linear-array transducers, such as U5-15LE (center frequency, 7.3 MHz) [37,38], eL18-4 (4-18 MHz), and L11-3U (11 MHz) or L9-3U (9 MHz) [39]. Regarding image acquisition parameters, the sampling frequency is generally set at 100 Hz [35,38,40], with a typical acquisition duration of 15 s per scan [35,37,38,40]. To minimize destruction of contrast microbubbles by the ultrasound beam, most studies have employed a relatively low mechanical index (MI), ranging from 0.06 to 0.1 [35,38-40]. SonoVue® has been used as the contrast agent in most studies [35,37-40], although the injection route varies according to the study purpose: conventional intravenous bolus injection is generally used for imaging the blood supply of breast tumors, whereas intradermal injection is used for sentinel lymph node imaging, with 0.5 mL injected at each of the 3, 6, 9, and 12 o'clock positions around the areola [40]. Because these acquisition parameters differ across studies and scanner platforms, no globally unified protocol or region of interest(ROI) standard has yet been established for breast SRUS, which limits multicenter reproducibility. Leveraging its ultra-high spatial resolution, ULM can effectively identify substantial differences in microvascular architecture and hemodynamics between benign and malignant lesions. A prospective study demonstrated that, morphologically, benign lesions predominantly exhibited punctate, linear, or branching microvascular patterns (93%), whereas malignant lesions were mainly characterized by disorganized microvascular networks (94%, $P < 0.001$).

Regarding quantitative parameters, microvascular density, mean diameter, maximum diameter, and maximum tortuosity were all significantly higher in malignant lesions than in benign lesions, whereas the mean blood flow velocity was significantly lower (all $P < 0.05$). Among these parameters, the maximum vascular diameter showed the best diagnostic performance for differentiating benign and malignant lesions, with an AUC of 0.962, a sensitivity of 88.2%, and a specificity of 92.9% [39]. Hou et al. further demonstrated, in a study involving 120 BI-RADS category 4 breast lesions, that maximum blood flow velocity, tortuosity, and complexity were independent predictors of malignancy, with tortuosity and complexity also showing utility in differentiating malignant lesions from hypervascular benign lesions. A nomogram model constructed based on SRUS parameters achieved an AUC of 0.899 for differentiating benign and malignant lesions, with a sensitivity of 94.3% and a specificity of 76.5%, and an AUC of 0.816 for differentiating malignant lesions from hypervascular benign lesions, with a specificity of 88.6%. Both models significantly outperformed conventional CDFI and superb microvascular imaging (SMI) techniques [37]. These findings indicate that quantitative SRUS features may help refine risk stratification of BI-RADS category 4 lesions and could reduce unnecessary biopsy in selected cases; prospective multicenter validation is still needed of hypervascular benign lesions.

Furthermore, SRUS has also been extended to the assessment of the tumor microenvironment and lymphatic system. Hua et al. applied SRUS to imaging the tumor interstitial-lymphatic network (ILN). The study showed that, compared with benign tumors, the ILN of malignant tumors exhibited lower vascular density, blood flow velocity, and vascular proportion, with more frequent peripheral and heterogeneous distribution and a lack of branching structures. Meanwhile, the complexity, maximum curvature, and vessel diameter of the ILN were significantly lower in malignant tumors, whereas the mean long-axis spacing was significantly greater [38]. Xia et al. further applied SRUS to achieve high-resolution imaging of lymphatic sinuses within breast sentinel lymph nodes (SLNs) at the 10-μm scale, while simultaneously extracting parameters including perfusion defects, lymphatic sinus density, intersinus spacing, and lymphatic flow velocity. The study demonstrated that SRUS achieved an AUC of 0.824 for predicting SLN metastasis, significantly higher than that of conventional ultrasound (AUC of 0.661) and conventional contrast-enhanced ultrasound (AUC of 0.714). Multivariate analysis indicated that perfusion defects (OR = 15.096), decreased mean sinus density throughout the lymph node (OR = 7.971), and increased maximum intersinus spacing in the cortical region (OR = 7.33) were independent predictors of SLN metastasis [40]. This approach may offer a new route to noninvasive preoperative assessment of breast cancer SLNs, pending validation in larger prospective cohorts.

Quantitative ultrasound imaging

Ultrasound Elastography Breast lesions exhibit heterogeneity not only in macroscopic and microscopic

清華大學出版社 Tsinghua University Press | SciOpen

morphology and vasculature, but also in the intrinsic mechanical properties. Ultrasound elastography is a non-invasive quantitative imaging technique for assessing the biomechanical properties of tissues. Its fundamental principle is to estimate tissue stiffness by measuring the strain or deformation response of tissues under external compression or internal acoustic force, or by detecting the propagation velocity of shear waves within tissues. Under pathological condition, breast cancer tissues are generally stiffer than normal breast tissues. This tissue stiffening is primarily regulated by the tumor microenvironment (TME) and results from abnormal deposition of extracellular matrix (ECM) proteins, which subsequently leads to increased ECM stiffness caused by collagen fiber remodeling [41]. These microscopic pathological alterations provide a robust biomechanical basis for the use of ultrasound elastography in further characterizing the mechanical properties of benign and malignant breast lesions. Currently, the main breast ultrasound elastography techniques include strain elastography (SE) and acoustic radiation force impulse (ARFI) imaging. According to the spatial extent of measurement, ARFI can be further classified into point shear wave elastography (pSWE), two-dimensional shear wave elastography (2D-SWE), and three-dimensional shear wave elastography (3D-SWE).

Breast US elastography is routinely performed using high-frequency linear-array transducers, although the image acquisition requirements vary across different elastography modes. For SE imaging, the acquisition plane should simultaneously include the lesion, subcutaneous adipose tissue, and the deep pectoralis major muscle. The target lesion should account for no more than 25% of the total ROI, and at least 5 mm of adjacent normal tissue should be included as a reference for stiffness comparison [42,43].

For shear wave elastography (SWE) imaging, the elasticity scale is typically displayed in kilopascals (kPa) to indicate Young's modulus, with the maximum scale commonly set at 175-180 kPa [44,45]. Some studies have instead directly quantified the parameters using shear wave velocity (m/s) [46-48]. In terms of scanning technique, SWE requires the operator to maintain light contact between the transducer and the skin without applying probe pressure and to instruct the patient to hold their breath, thereby minimizing precompression artifacts. For quantitative measurements, the ROI is typically set as a circular region and placed within the stiffest area of the lesion. In some rigorous study protocols, three ROIs are placed in both the stiffest and softest regions of the lesion, while a quality control map (SW-quality map) is used to exclude areas with a low signal-to-noise ratio, thereby ensuring the reliability of shear wave velocity (SWV) measurements [46]. These variations in acquisition standards highlight the necessity of establishing and strictly adhering to standardized elastography parameters and acquisition protocols in clinical implementation and multicenter studies.

Built-in imaging analysis algorithms are crucial for quantitative imaging, current technologies for SWE are also undergoing continuous evolution and optimization. When faced with breast lesions characterized by a low signal-to-noise ratio or extremely low echogenicity and high stiffness, the conventional standard algorithm is prone to generating "soft cancer" artifacts due to severe shear wave attenuation, whereby extremely stiff malignant lesions are erroneously interpreted as soft tissue, resulting in false-negative findings. To address this technical bottleneck, Barr et al. developed and validated a novel algorithm, which substantially overcomes this limitation by optimizing the detection mechanism and quality discrimination logic of shear waves. The results showed that the sensitivity of their algorithm for diagnosing malignant breast lesions increased markedly from 45% with using standard algorithms to 100%, while maintaining a specificity of 81% [48]. If confirmed prospectively, this algorithmic improvement may help reduce unnecessary biopsies in a proportion of BI-RADS category 4 lesions.

Viscoelastic Elastography Ultrasound viscoelasticity imaging (viscoelastic elastography) is an advanced quantitative imaging technique based on shear waves. Conventional SWE generally idealizes tissues as purely elastic media and assumes that shear waves propagate at a constant velocity, thereby assessing tissue stiffness alone. However, real biological tissues are complex "viscoelastic media" that exhibit both elastic and viscous properties. In viscoelastic media, the propagation velocity of shear waves varies with frequency, a phenomenon known as dispersion, while the wave amplitude also rapidly attenuates due to viscous dissipation caused by internal friction [49]. Therefore, simply disregarding the viscous properties of tissues not only results in the loss of critical pathological information but may also lead to simplified assessment of lesion characteristics. To more comprehensively and accurately characterize the biomechanical and pathological states of tissues, ultrasound viscoelasticity imaging has emerged as a promising approach. Currently, several advanced techniques, including shear wave dispersion ultrasound vibrometry (SDUV) [50], Viscoelastic Response Imaging(VisR) [51], and shear wave dispersion imaging (SWD) [52-54], have been developed for the noninvasive quantitative assessment of tissue viscous properties.

In the clinical practice of breast ultrasound viscoelasticity imaging, high-frequency linear-array transducers

are typically used, with broadband frequency ranges of 3-11 MHz [53,55] or 5-18 MHz [54], to ensure adequate spatial resolution. Similar to conventional elastography, quality control during measurement and standardized setting of ROI are essential for ensuring data reliability. Currently, different studies have adopted diverse strategies for standardizing image acquisition and measurement. Some studies have manually delineated the lesion contours with precision [53,56], or systematically sampled characteristic regions of color viscoelasticity maps using a fixed-size quantitative box (Q-Box) [55]. Other more refined studies have further defined the lesion core, peritumoral region, and distal normal tissue reference region, and performed multidimensional independent measurements by placing multiple ROIs [57], while introducing specific indices, such as the M-STB index, for rigorous image quality filtering. The heterogeneity in measurement parameters and sampling strategies further highlights the urgent need to establish standardized protocols for ultrasound viscoelasticity imaging in future clinical implementation and multicenter studies.

Ultrasound Image Analysis: From Manual to AI-Driven

Quantitative analysis of ultrasound images are instrumental for achieving precise assessment of breast lesions. With technological advances, quantitative analysis has evolved from simple quantifications of tissue (micro)vasculature, elasticity and viscosity based on reconstructed B-mode images toward the in-depth extraction of high-dimensional radiomic features directly from raw ultrasound radiofrequency (RF) signals.

Quantitative analyses

Microflow Analysis In morphological assessment, the microvascular architecture (VA) of breast lesions can be classified into five types: type I, avascular; type II, punctate and linear; type III, branching; type IV, root-like; and type V, crab-claw-like [58]. Among these, the vascular patterns of the avascular, punctate and linear, and branching types are relatively regular and are more commonly observed in benign lesions, whereas the root-like and crab-claw-like types are more closely associated with malignant tumors [58]. In quantitative analysis, SMI can objectively assess the blood supply of breast masses using the vascular index (VI). A meta-analysis showed that VI achieved an AUC of 0.81 for the diagnosis of malignant breast lesions, indicating moderate diagnostic accuracy [59]. Lee et al. evaluated the reproducibility and auxiliary diagnostic value of this index. The results showed excellent intraobserver and interobserver agreement for VI (intraclass correlation coefficient [ICC] = 0.960 and 0.948, respectively), which was not affected by lesion characteristics. The addition of VI to B-mode ultrasound BI-RADS assessment significantly improved both diagnostic specificity and the κ value for diagnostic agreement ($P < 0.05$) [27].

Multiple studies have further explored the clinical value of VI and its optimal cutoff values. Cai et al. found that VI values were significantly higher in malignant lesions than in benign lesions, with a cutoff value of 4.05%. After incorporating SMI parameters (VI ≥ 4.05% or type IV/V VA) with conventional ultrasound for downgrading BI-RADS category 4 lesions, the combined model achieved an AUC of 0.941, significantly higher than that of conventional ultrasound alone ($P < 0.001$) [29]. Lee et al. reported a similar VI cutoff value of 3.35%, but noted that SMI may carry a certain risk of false-negative results in small lesions measuring < 10 mm in diameter, pure ductal carcinoma in situ, or low-grade invasive carcinomas. Therefore, SMI should be applied with caution in clinical practice [60].

In addition to differential diagnosis, recent studies have also explored the use of SMI combined with shear wave elastography for the early prediction of therapeutic response to neoadjuvant chemotherapy (NAC) in breast cancer. Zuo et al. enrolled 107 patients with invasive breast cancer and used color SMI (cSMI) and monochrome SMI (mSMI) to measure the vascular index and assess lesion extent. The results showed that after two cycles of chemotherapy, the change rate of VI (ΔVI%) was significantly higher in the pathological complete response (pCR) group than in the non-pCR group ($P < 0.001$), and ΔVI% was identified as one of the independent predictors of pCR (OR = 1.034, $P = 0.015$) [30]. In contrast to the ΔVI%, a retrospective study involving 88 patients evaluated the predictive value of multiparametric ultrasound for pCR after NAC and found that baseline SMI vascular index was slightly higher in the pCR group than in the non-pCR group (8.07% vs. 6.08%), with no statistically significant difference ($P = 0.134$); baseline vascular index was not an independent predictor of pCR [28]. Such discrepancies may be attributable to differences in patient inclusion criteria, device parameters, ROI definition, and biases inherent in the original studies; prospective multicenter validation is therefore warranted.

In the prediction of molecular subtypes of breast cancer, one study found that the mean VI was significantly higher in non-luminal subtypes, including HER2-overexpressing and triple-negative breast cancer, than in luminal subtypes ($P = 0.002$) [61]. Zhang et al. further demonstrated that although the overall difference in VI among the five molecular subtypes was not statistically significant, VI showed relatively high sensitivity for pre-

清華大學出版社 Tsinghua University Press | SciOpen

dicting the Luminal A subtype (79.9%, cutoff value 4.1%) and relatively high specificity for predicting triple-negative breast cancer (90.3%, cutoff value 16.4%) [31]. The above findings suggest that the microvascular index VI may reflect the biological aggressiveness of breast tumors to some extent, but its ability to differentiate molecular subtypes as a single parameter remains relatively limited.

Quantitative Elastography Analysis SE primarily assesses tissue stiffness under manual compression using semiquantitative parameters, including the EI/B ratio and Tsukuba elasticity score. For example, Kanagaraju et al. [62] used SE semiquantitative parameters, including the elasticity-to-B-mode area ratio (EI/B ratio) and the Tsukuba elasticity score to evaluate breast lesions and found that the mean EI/B ratio was significantly higher in malignant lesions (1.36 ± 0.24) than in benign lesions (1.03 ± 0.30). SE substantially increased the specificity of BI-RADS assessment from 9.5% to 76.1%, effectively enabling the downgrading of some BI-RADS category 4 lesions [42]. A large prospective study involving 1, 288 lesions further evaluated the combination of SE and SWE, using cutoff values of SWE ≥ 3.70 m/s and SE E/B ≥ 1. The results showed that combined assessment reduced the relative rate of unnecessary biopsies following conventional ultrasound by 35.35%, with an overall sensitivity of 96.7% and a specificity of 65.2% [63]. SWE, such as ARFI-based techniques, generates shear waves through acoustic radiation force and can directly provide quantitative measurements of the Young's modulus of lesions, including the mean elasticity (Emean), maximum elasticity (Emax), minimum elasticity (Emin), and standard deviation (Esd) [62]. Although SWE is less operator-dependent and exhibits good reproducibility, studies by Tekcan Sanli et al. and Li et al. have indicated that nonpathological factors, such as lesion size, depth, and margin morphology, may exert confounding effects on the measurements. Therefore, these parameters should be interpreted in conjunction with two-dimensional ultrasound findings for comprehensive clinical assessment [47,64].

Numerous studies have demonstrated that SWE parameters are closely associated with the biological aggressiveness of breast cancer. Tumors with higher histological grades, vascular invasion, high Ki-67 expression [64], as well as those presenting as invasive carcinoma, triple-negative breast cancer, or axillary lymph node-positive disease, exhibit significantly higher SWE quantitative parameters ($P < 0.05$) [65]. The role of SWE in therapeutic response prediction has also been investigated. For example, Zhao et al. investigated the predictive value of SWE for the efficacy of neoadjuvant chemotherapy (NAC) and found that the elasticity modulus was significantly lower in the pathological complete response (pCR) group than in the non-pCR group. A model incorporating SWE parameters, Ki-67, and molecular subtypes achieved an AUC of 0.922 for predicting pCR [45].

Regarding quantitative assessment of viscosity, ultrasound viscoelasticity imaging further enriches the biomechanical characterization of tissues. The shear viscosity coefficient (η, Pa·s) extracted based on the Voigt model and its derived relaxation time constant (τ) can reflect the rate at which tissues recover to an equilibrium state following mechanical deformation [66,67]. Studies have shown that the dispersion slope (typically > 20 (m/s)/kHz) and viscosity coefficient are significantly higher in malignant breast lesions than in benign lesions, suggesting that invasive carcinoma and ductal carcinoma in situ exhibit high-viscosity characteristics [52,54]. Woo et al. compared SWD with SWE and found that the mean tumor dispersion value (D-tumor) achieved an AUC of 0.96 for the diagnosis of malignancy, with particularly excellent performance in small lesions measuring ≤ 20 mm, suggesting that viscosity-related parameters can capture biological differences that are difficult to reflect using conventional elastography [52]. Xu et al. further focused on the peritumoral viscoelastic characteristics and found that peritumoral viscoelastic parameters allowed downgrading of 69 of 73 BI-RADS category 4 benign lesions, outperforming elasticity or viscosity parameters alone in this retrospective cohort [57]. Furthermore, viscosity-related parameters are also closely associated with tumor proliferation and the inflammatory microenvironment. Tao et al. found that, in invasive ductal carcinoma, the mean viscosity coefficient was significantly lower in the high Ki-67 expression group than in the low-expression group [56]. Yang et al. constructed a model combining viscoelastic parameters with systemic inflammatory indicators, which achieved an AUC of 0.934 for differentiating benign and malignant lesions [55].

Radiofrequency Signal Analysis Ultrasound radiofrequency (RF) signals are raw echo data received by the transducer before post-processing. Compared with B-mode images generated through logarithmic compression and envelope detection, RF signals retain the complete amplitude, phase, and frequency information arising from the interaction between ultrasound waves and underlying tissues. Although the clinically used delay-and-sum (DAS) reconstruction algorithm meets the requirements of real-time imaging, its limited signal-to-noise ratio results in the loss of substantial microscopic information. To address this limitation, Zhang et al. proposed an RF data reconstruction method based on a self-supervised deep neural network, which

employs a composite loss function incorporating wavelet-domain sparsity and reduces the reconstruction time to less than 10 ms with a single plane-wave transmission, thereby substantially improving the clinical feasibility of high-quality RF imaging [68].

Direct extraction of quantitative features from RF signals has opened a new avenue for the microscopic characterization of breast cancer. Ouyang et al. constructed H-scan images by mapping the low-frequency components, representing large scatterers, and high-frequency components, representing small scatterers, of RF signals. They found that malignant tumors exhibited prominent blue signals, reflecting the presence of small scatterers, effectively complementing the microscopic structural heterogeneity concealed in B-mode ultrasound [69]. Wang et al. performed bispectral analysis of RF signals and constructed four frequency-segmented energy feature maps, confirming that the high- and low-frequency feature maps contributed most to lesion classification [70]. To achieve synergistic integration of multimodal information, a study extracted the H-scan color scale, Burr distribution parameters, and morphological features from RF signals and generated a color-coded "malignancy probability overlay map" based on a machine learning framework. The resulting approach achieved a diagnostic accuracy of over 98% in a single-center retrospective dataset, outperforming BI-RADS scoring in that dataset [71]. For challenging BI-RADS category 4 lesions, Xie et al. proposed a spectral analysis enhancement network (SAE-Net) that integrates the continuous wavelet transform spectrum of RF signals with grayscale morphological features. While maintaining a sensitivity of 95%, the model would have allowed 43.3% of benign lesions to avoid biopsy in that dataset [72]. Notably, to address the clinical challenge of limited access to raw RF data, one study successfully employed a deep generative adversarial network (ViT cGAN) to inversely synthesize highly reconstructed RF signals from conventional B-mode images, achieving a lesion classification accuracy of 82% based on quantitative ultrasound (QUS) features extracted from the synthesized RF signals. This breakthrough may help overcome the barrier to accessing raw data and accelerate the clinical adoption of QUS analysis [73]. These findings await validation in independent external cohorts before they can be translated into clinical practice.

Computer-aided diagnosis

Representative AI and computer-aided di-agnosis (CAD) studies are summarized in table 1. Unlike traditional manual image interpretation, which relies heavily on radiologists' experience and is subject to interobserver variability, computer-aided diagnosis and artificial intelligence technologies can deeply mine high-dimensional latent features that are difficult to perceive by the human eye. The application of AI not only facilitates the detection of small and otherwise occult lesions but also substantially reduces interobserver cognitive variability, thereby improving the objectivity and consistency of image interpretation. A large body of research has comprehensively validated the clinical value of AI-assisted breast ultrasound diagnosis from multiple perspectives. Such tools are intended to assist radiologists and clinicians in triage and risk stratification rather than to replace histopathological diagnosis as the gold standard. At the same time, it should be noted that most of these models were derived from retrospective studies, and the high AUCs obtained in internal validation often decrease to varying degrees in independent external cohorts; exploratory model performance should therefore be distinguished from real-world clinical utility.

At the clinical application level, Zhao et al. developed a deep learning model based on breast ultrasound videos (DL-video), which achieved an AUC of 0.969, significantly higher than that of the static image-based model (DL-image; AUC of 0.925; $P = 0.0172$) and that of six radiologists (AUC of 0.779-0.912; $P < 0.05$) [32]. Moreover, all six radiologists demonstrated better diagnostic performance when interpreting dynamic videos than when interpreting static images [32]. Wei et al. evaluated a commercially available deep learning-based CAD system, such as S-Detect. The results showed that the system achieved a diagnostic accuracy, sensitivity, and specificity of 89.6%, 94.2%, and 87.0%, respectively, on the long-axis view of lesions. Using BI-RADS category 4a as the threshold, the system achieved an AUC of 0.906, significantly outperforming both experienced radiologists (0.734) and less experienced radiologists (0.696), thereby effectively reducing the rate of unnecessary biopsies [74]. Gu et al. also demonstrated that the performance of CAD in BI-RADS categorization did not differ significantly from the consensus assessment of experienced experts. Notably, CAD showed substantial potential for downgrading BI-RADS category 4a lesions: in external validation, 63.49% of category 4a lesions were safely downgraded to category 3 without any missed malignant lesions [75].

With more and more clinical US data becoming accessible, this has also enabled development of large-scale deep learning models. For instance,Shen et al. trained an AI diagnostic model using approximately 5.44 million ultrasound images from 143, 000 patients, encompassing a total of 289, 000 examinations. The model achieved an AUC of 0.976 on an independent test set. In a comparative study involving image interpretation by 10 breast radiologists, the AI achieved an AUC

清華大學出版社 Tsinghua University Press | SciOpen

Table 1 Summary of representative AI/CAD models for breast ultrasound diagnosis

Author	Year	Country	Model and architecture	Study design	Centers	Input	No. of cases	Age (years)	Task	AUC	External-validation status
Wei et al. [74]	2022	China	S-Detect (deep-learning CAD)※	Prospective	9	B-mode	901	45.2 ± 10.8	Differentiation of benign and malignant breast masses	0.906	YES
Gu et al. [75]	2023	China	DL-BI-RADS (RepVGG)	Prospective	32	B-mode	5,012	44.1 ± 13.1	Benign/malignant classification and 6-category BI-RADS	0.980	YES
Shen et al. [76]	2021	United States	Breast ultrasound AI (attention mechanism)	Retrospective	20	B-mode + Color Doppler	143,203	53.7 ± 13.7	Breast cancer detection and triage of low-risk examinations	0.976	YES
Mango et al. [77]	2020	United States	Koios DS※	Retrospective	> 20	B-mode	900	53.6	Lesion risk stratification and management recommendations	0.88	YES
Lai et al. [78]	2022	Taiwan, China	BU-CAD (deep-learning CAD)※	Retrospective	1	B-mode	172	54.1 ± 12.0	Lesion detection and diagnosis	0.859	NO
Chen et al. [79]	2025	China	AINet	Retrospective	7	B-mode + SWE	15,223	N/A	Benign/malignant classification and BI-RADS grading	0.942	NO
Cai et al. [80]	2025	International	AI-SWE (EfficientNetB1)	Retrospective	12	SWE	1,294	46.5 ± 16.3	Benign/malignant stratification of BI-RADS 3/4 lesions	0.94/0.93	YES
Qian et al. [81]	2024	China	BMU-Net (ResNet-18 + Transformer)	Prospective	≥ 3	MMG + US (three-modal) + clinical	5,025	48.8	Coarse-/fine-grained breast cancer risk stratification	0.948	YES
Jiang et al. [82]	2021	China	ResNet50-DCNN	Retrospective	3	B-mode	2,120	49	Breast cancer molecular subtype classification	0.87/0.83	YES
Zhou et al. [83]	2020	China	Inception V3	Retrospective	2	B-mode	834	48	Prediction of axillary lymph node metastasis	0.89	YES

AI, artificial intelligence; AUC, area under the curve; BI-RADS, Breast Imaging Reporting and Data System; B-mode, grayscale ultrasound; BU-CAD, breast ultrasound computer-aided diagnosis; CAD, computer-aided diagnosis; CDFI, color Doppler flow imaging; DCNN, deep convolutional neural network; DL, deep learning; NR, not reported; SWE, shear wave elastography. ※Commercially available CAD system.

of 0.962, which remained significantly higher than the mean performance of the radiologists (0.924). Beyond its own excellent diagnostic performance, the "human-AI collaboration" model provided substantial benefits to clinicians. In this study, AI-assisted interpretation effectively reduced diagnostic errors among radiologists, with specificity increasing markedly from 80.7% to 88.0% [76]. A similar study by Mango et al. also found that, with AI assistance, the mean diagnostic AUC of 15 radiologists increased from 0.83 to 0.87, while interobserver agreement, measured by Kendall's τ-b, improved significantly from 0.54 to 0.68 [77]. Another study involving 16 radiologists by Lai et al. further demonstrated that AI not only improved diagnostic accuracy but also reduced the mean image interpretation time from 30.15 s to 18.11 s, representing an approximately 40% reduction in interpretation time. Notably, less experienced radiologists derived particularly substantial benefits from AI assistance [78].

Over the past decade, AI-assisted diagnosis has progressed from the analysis of single-modal US alone toward multimodal collaborative analysis that integrates complementary imaging information. Chen et al. performed deep alignment of B-mode ultrasound images with SWE features and developed the AINet, which significantly outperformed conventional unimodal methods in both benign-malignant classification and BI-RADS categorization tasks [79]. An AI-SWE multiparametric model developed by Cai et al. also demonstrated excellent performance in two external validation cohorts, reducing the false-positive rate by 62.1% and 38.1%, respectively, while maintaining sensitivity [80]. Qian et al. further expanded the dimensionality of the input data by developing the BMU-Net model, which deeply integrates three-modal ultrasound information, including B-mode ultrasound, color Doppler, and elas-

tography in both transverse and longitudinal views, bilateral mammographic views, and clinical metadata, such as age and body mass index (BMI). The coarse-grained accuracy, defined as the accuracy of binary benign-malignant classification, of this multimodal model reached 90.1%, approaching the level achieved by pathologists in the preliminary assessment of biopsy specimens (92.7%) [81].

Beyond benign-malignant differentiation, AI has also demonstrated emerging value in predicting breast cancer molecular subtypes and axillary lymph node (ALN) metastasis. A multicenter study developed a ResNet50-based model to predict four molecular subtypes (Luminal A, Luminal B, HER2-enriched, and triple-negative breast cancer) using pretreatment conventional ultrasound images. The four-class classification accuracy on the external test set ranged from 80.07% to 98.83%. Heatmaps generated by the model revealed significant subtype-specific differences in the regions of interest, suggesting that subtype-specific macroscopic phenotypes may be latent in breast ultrasound images [82]. Regarding ALN status assessment, another preoperative prediction study focusing on patients with clinically node-negative disease demonstrated that an Inception V3 model based on two-dimensional grayscale ultrasound achieved an AUC of 0.89 (95% confidence interval [CI]: 0.83-0.95) on the external test set, providing noninvasive information that may assist axillary surgical planning [83].

Application

Screening

Early screening of breast cancer is a critical step in reducing mortality and improving long-term outcomes. Currently, population-based screening primarily relies on mammography, with ultrasound serving as a complementary modality in selected populations. Guidelines from multiple countries recommend mammography as the preferred modality for population-based screening, although specific screening strategies vary. The United States Preventive Services Task Force (USPSTF) recommends biennial mammographic screening, considering this interval to provide an optimal benefit-risk balance in reducing false-positive findings and overdiagnosis [84]. In contrast, the European Society of Breast Imaging (EUSOBI) and the China Anti-Cancer Association recommend personalized screening strategies based on age and individual risk stratification [85,86]. A meta-analysis involving 124, 425 Asian women showed that the pooled sensitivity of mammography was significantly higher than that of ultrasound (0.81 vs 0.65, P = 0.03), whereas no significant difference was observed in specificity [87]. However, the sensitivity of mammography is reduced in women with dense breasts. Owing to the high-density masking effect caused by overlapping glandular tissue, the sensitivity of mammography alone for screening dense breasts is only approximately 50% [88,89]. In addition, dense breasts are associated with a higher incidence of malignant tumors than fatty breasts, with studies indicating that the risk of breast cancer may be more than four times higher in women with dense breasts [89].

As an important adjunctive screening modality, ultrasound offers the advantages of being free of ionizing radiation, cost-effective, and convenient. Through dynamic multiplanar scanning, it can clearly delineate lesions by exploiting differences in acoustic impedance between malignant lesions and dense glandular tissue, while also identifying microscopic structures such as the ductal-lobular unit, thereby effectively compensating for missed diagnoses caused by tissue overlap on mammography. In women with dense breasts, ultrasound can further facilitate risk stratification through assessment of glandular tissue composition (GTC), thereby enabling more precise identification of women with high GTC who may benefit from supplemental ultrasound screening [88]. Harada-Shoji et al. systematically evaluated the clinical benefit of supplemental ultrasound screening based on the Japan Strategic Anti-cancer Randomized Trial (J-START), and found that the sensitivity of combined mammography plus ultrasound was significantly higher than that of mammography alone (93.2% vs 66.7%, $P < 0.001$), while the incidence of interval cancer was significantly reduced (0.5/1,000 vs 2.0/1,000, $P = 0.004$). Furthermore, among women with dense breasts, the proportion of invasive cancers detected by ultrasound alone was significantly higher than that detected by mammography (82.4% vs 41.7%), suggesting that ultrasound may have greater sensitivity for detecting early invasive lesions [90].

Although hand-held conventional ultrasound has demonstrated substantial value in breast cancer screening, its performance is highly operator-dependent and its image reproducibility is limited. To address these limitations, automated breast ultrasound (ABUS) was developed. Driven by a computer-controlled mechanical arm, ABUS automatically scans the entire breast, physically separating image acquisition from physician interpretation and thereby greatly facilitating remote consultation and standardized quality control. Multiple studies have demonstrated the efficiency of ABUS in population-based screening. Güldoğan et al. found that ABUS significantly reduced physician interpretation time, with an average saving of approximately 2.6 min per case

清華大學出版社 Tsinghua University Press | SciOpen

(158.44 s), while its standardized scanning time remained relatively constant regardless of differences in breast density [91]. In terms of detection performance, a study by Klein Wolterink et al. focusing on women with dense breasts reported a cancer detection rate of 2.77/1,000, a recall rate of 5.2%, and a biopsy rate of 1.8% with supplemental ABUS screening [92]. Gatta et al. were the first to report prone-position ABUS. After combining prone ABUS with mammography to screen 1,165 women with dense breasts, the supplemental cancer detection rate reached 3.4/1,000, increasing the overall sensitivity substantially from 58.8% to 93.5%. Notably, prone-position ABUS uses the same patient positioning as breast MRI, not only providing superior spatial resolution and image contrast but also greatly facilitating spatial registration and "second-look" comparison between ultrasound and MRI images [93]. In addition, Park et al. developed a low-cost three-dimensional (3D) ABUS system that demonstrated good image quality and ease of operation in healthy volunteers; however, its diagnostic performance in real-world breast cancer screening settings remains to be further validated in large-scale clinical studies [94].

Oncological diagnosis

Unlike large-scale screening of asymptomatic populations, in patients with clinically detected breast abnormalities, multimodal ultrasound imaging plays an indispensable central role in the precise characterization of tumors, risk stratification, and regional lymph node assessment.

In the risk stratification of breast masses, the multimodal approach combining conventional ultrasound with SWE and CEUS is the most widely used. Shen et al. demonstrated that the combination of conventional ultrasound, CEUS, and SWE achieved a diagnostic AUC of 0.877 and safely downgraded 55.8% of BI-RADS category 4A masses to category 3, with no missed malignant lesions confirmed by pathology [95]. A further study by Li et al. showed that the combination of the three modalities achieved an AUC of 0.946, significantly outperforming each single-modality or two-modality combination (all $P < 0.05$). These findings suggest that the integrated assessment of two-dimensional morphological features, microvascular perfusion, and biomechanical stiffness may help refine the triage of challenging BI-RADS category 4 lesions [96]. Furthermore, replacing CEUS with the completely noninvasive SMI in combination with SWE has also demonstrated excellent diagnostic performance for differentiating breast lesions [60,97]. For breast non-mass lesions (NMLs), which are more challenging to diagnose, Yang et al. developed a comprehensive assessment approach integrating conventional ultrasound, MVFI, SWE, and CEUS. The results showed that this approach achieved a Kappa value of 0.806 for agreement with pathological findings and a diagnostic AUC of 0.922, significantly outperforming any single diagnostic modality ($P < 0.05$) [98].

Accurate assessment of regional lymph node status in breast cancer is directly related to the selection of surgical approaches and long-term prognosis. However, the sensitivity of conventional ultrasound and CDFI alone is limited, creating an urgent clinical need for more effective noninvasive approaches to guide decisions regarding SLN biopsy. Against this background, CEUS, with its ability to dynamically visualize lymphatic vessels and the microcirculatory perfusion characteristics of lymph nodes, provides an important complementary approach for the noninvasive assessment of regional lymph node metastasis in breast cancer. Niu et al. systematically analyzed the intradermal CEUS features of sentinel lymph nodes (SLNs) in breast cancer and reported that homogeneous enhancement (type I) and characteristic heterogeneous enhancement (type II) yielded a negative predictive value of 91.7% for axillary-negative SLNs, whereas SLNs exhibiting focal defects (type III) and no enhancement (type IV) had metastasis rates of 65.2% and 57.1%, respectively. The study demonstrated that CEUS achieved significantly better diagnostic performance for SLN metastasis than conventional ultrasound (AUC of 0.813 vs. 0.601; $P < 0.001$), providing reliable imaging evidence for the preoperative noninvasive assessment of axillary lymph node status [99]. Zhuang et al. found that CEUS performed through intradermal injection into the subcutaneous lymphatic vessels achieved a sensitivity of 86.2%, a specificity of 95.0%, and an AUC of 0.906 for diagnosing SLN metastasis, whereas the addition of conventional intravenous CEUS provided no further diagnostic benefit [100]. In the field of radiomics and AI, a multicenter study extracted radiomic features from grayscale ultrasound, CDFI, and contrast-enhanced ultrasound (CEUS) to predict ALN metastasis. The multimodal model achieved AUCs of 0.88, 0.81, and 0.77 in the training, internal validation, and external validation sets, respectively, significantly outperforming the corresponding AUCs of 0.81, 0.71, and 0.71 achieved by the grayscale ultrasound model alone (all $P < 0.05$). When further differentiating low-burden metastasis (1-2 metastatic nodes) from high-burden metastasis (≥ 3 metastatic nodes), the multimodal model achieved an AUC of 0.75 in the external validation set, which was also significantly higher than that of the ultrasound-only model (0.61, $P < 0.05$) [101]. Huang et al. developed a bimodal deep learning model based on grayscale ultrasound and CEUS, which achieved an

AUC of 0.912 in internal testing and demonstrated strong generalizability across three prospective multicenter external cohorts, with AUCs of 0.893, 0.866, and 0.862, respectively [102]. In addition, another study adopted a different approach by directly constructing a predictive model based on multimodal features of the primary breast lesion, including multifocal/multicentric distribution, architectural distortion, microcalcifications, and the SWE halo sign, to assist in predicting ALN metastasis. The combined model achieved an AUC of 0.803 (95% CI: 0.739-0.867), significantly outperforming either B-mode ultrasound or SWE alone [103].

Although multimodal ultrasound and advanced intelligent algorithms have demonstrated excellent performance in the diagnosis and staging of breast cancer, some studies remain limited by single-center designs or insufficient sample sizes, and their generalizability urgently requires validation in large-scale, prospective multicenter cohorts. Therefore, in current clinical practice, multimodal ultrasound is more appropriately positioned as an advanced adjunctive tool for pre-biopsy or preoperative risk stratification rather than as a substitute for pathological diagnosis as the gold standard. Representative multimodal ultrasound features of benign and malignant breast lesions are shown in figure 2.

Beyond US Radiomics: From Radiogenomics to Radio-multiomics

The aforementioned studies have demonstrated that breast ultrasound can characterize tumor phenotypes across multiple dimensions, including morphology, blood flow, microvasculature, and tissue biomechanics, while radiomics and AI further enable quantitative analysis. The next step in its development is not simply to increase the number of imaging features but rather to establish associations between these reproducible imaging phenotypes and the molecular and cellular characteristics of tumors, thereby narrowing the scale gap between “macroscopic imaging” and “microscopic biology” [104,105].

Radiogenomics

Currently, the integration of ultrasound imaging with molecular information has primarily focused on radiogenomics. Xi et al. analyzed 777 breast tumor samples with both ultrasound radiomics and whole-genome sequencing data and identified cross-modal association modules from 846 ultrasound radiomic features and 553 mutated gene features, suggesting systematic associations between ultrasound phenotypes and cancer driver genes and related signaling pathways [106]. Regarding specific molecular biomarkers, ultrasound radiomics has been used to predict HER2 status, achieving an AUC of 0.80. Microvascular ultrasound parameters have also been shown to be associated with genetic alterations in angiogenesis-related genes, while studies of triple-negative breast cancer (TNBC) have further suggested associations between ultrasound imaging features and signaling pathways, including JAK-STAT, MAPK, RAS, Wnt, and PI3K-AKT [107-109].

It is worthwhile noting that these radiogenomic findings should be interpreted with caution. Associations between radiomic features and molecular markers may be driven by confounders such as tumor size, cellularity, and fibrosis, which can simultaneously influence gene expression and image texture. Most inferences are also unidirectional, reflecting how imaging phenotypes correspond to molecular states without explaining how molecular alterations give rise to specific imaging appearances. Moreover, any single molecular layer reflects only one biological scale and cannot fully capture intratumoral heterogeneity.

Radio-multiomics

Compared with associations between imaging phenotypes and single molecular layers, multi-omics integration enables the incorporation of information across different biological scales. At present, studies directly integrating ultrasound with molecular omics remain limited, among which the study by Yang et al. is particularly representative. Among 1,723 participants who underwent automated breast volume scanning (ABVS), 238 pathologically confirmed breast nodules were analyzed using an integrated approach combining breath metabolomics and ultrasound radiomics. The breath-omics model alone achieved an AUC of 0.855, whereas the AUC increased to 0.946 after integrating breath metabolomics, ultrasound radiomics, and clinical information, with a sensitivity and specificity of 84.1% and 89.9%, respectively, based on five-fold cross-validation [110]. Such results highlight the complementary value of ultrasound-derived spatial phenotypes and systemic metabolic information, while representing an early form of imaging–metabolomics integration rather than multi-omics integration.

Beyond conventional multi-omics, spatial multi-omics may provide further insights by linking imaging phenotypes with the spatial distribution of molecular and cellular features within tumors. Integrating spatial transcriptomics, digital pathology, and protein profiling may help characterize intratumoral heterogeneity and the tumor microenvironment. However, its application in ultrasound-based radio-multiomics remains a prospective research direction requiring spatially matched imaging and tissue data for validation.

清華大學出版社 Tsinghua University Press | SciOpen

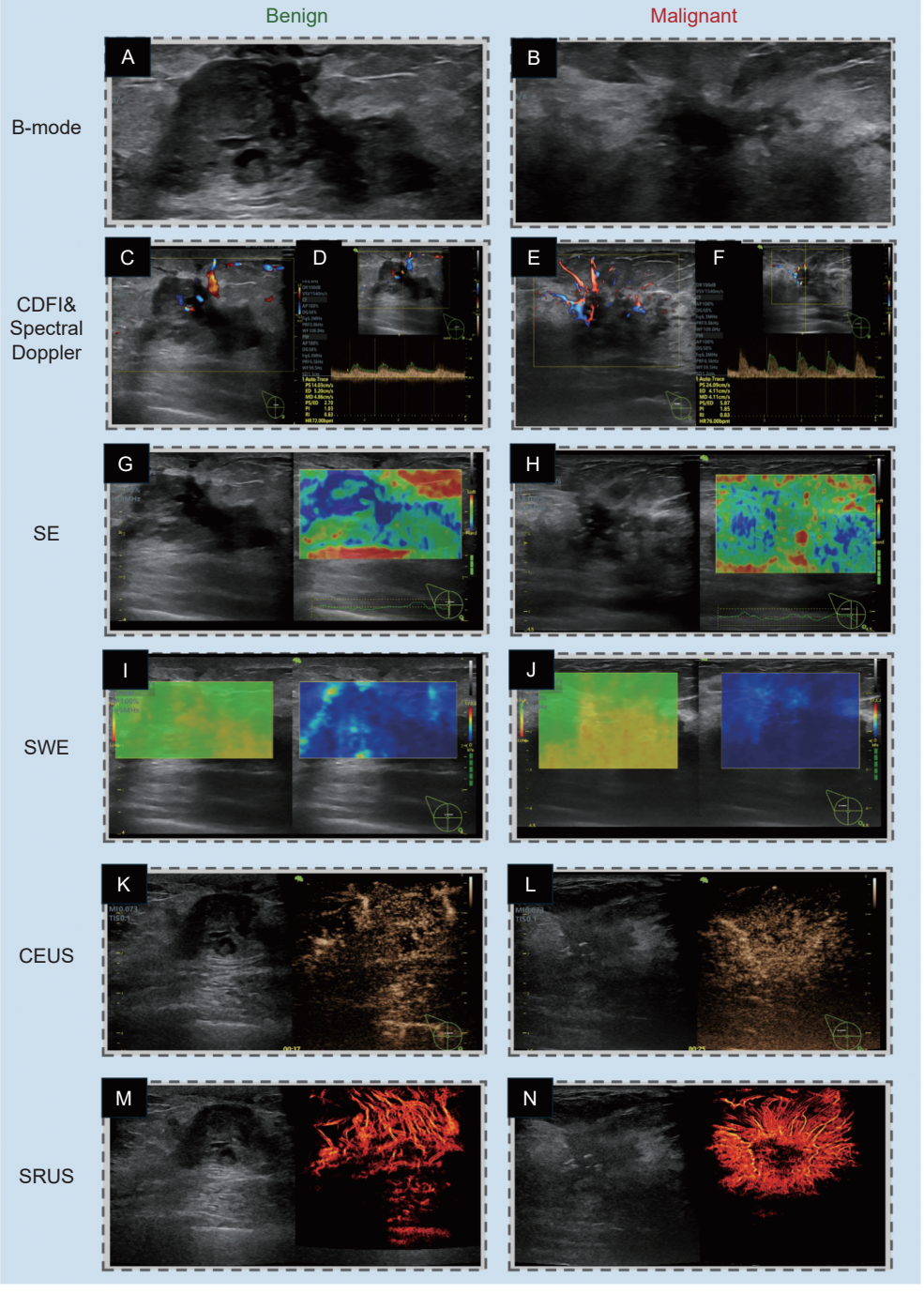


Figure 2 Comparison of multimodal ultrasound imaging features between benign and malignant breast lesions. (A, B) B-mode ultrasound; (C, E) color Doppler flow imaging; (D, F) spectral Doppler; (G, H) strain elastography; (I, J) shear wave elastography; (K, L) contrast-enhanced ultrasound; and (M, N) super-resolution ultrasound. The left column (A, C, D, G, I, K, M) shows the benign lesion, whereas the right column (B, E, F, H, J, L, N) shows the malignant lesion.

Much of the current evidence integrating radiomics with multiple molecular omics layers comes from MRI-based studies rather than ultrasound. The following studies should therefore be interpreted as methodological references for future ultrasound research, not as direct evidence of the clinical performance of ultrasound-based radio-multiomics. Jiang et al. integrated contrast-enhanced magnetic resonance imaging (CE-MRI) radiomics with transcriptomic, metabolomic, and clinical information to predict molecular subtypes of TNBC, and further linked imaging heterogeneity to an immunosuppressive tumor microenvironment and metabolic reprogramming [111]. Su et al. further demonstrated, in a multicenter cohort of 1, 474 patients, that intratumoral imaging heterogeneity was associated with genomic heterogeneity, tumor mutational burden, alterations in RAS/MAPK/PI3K-AKT-mTOR-related pathways, and metabolic changes [112]. These studies provide impor-

tant directional guidance for the future development of ultrasound, suggesting that research should move beyond the prediction of individual molecular biomarkers toward elucidating the molecular mechanisms underlying imaging phenotypes.

From a methodological perspective, the MVNMF framework, developed using dynamic contrast-enhanced MRI (DCE-MRI) and multiple genomic layers, illustrates how imaging features can be jointly modeled with molecular data [113]. This MRI-derived approach may inform future ultrasound research, but its transferability and performance require separate evaluation in ultrasound datasets. Ultrasound may offer an accessible imaging modality for non-invasive molecular phenotyping research. Nevertheless, studies directly integrating ultrasound with two or more molecular omics layers remain scarce [105,106,110].

Following established frameworks for multimodal and multi-omics integration, ultrasound–omics approaches can be broadly discussed in terms of feature-level (early), intermediate-level, and decision-level (late) fusion, according to the stage at which information is combined [114,115].

Feature-level (early) fusion combines extracted ultrasound, molecular, and clinical features before predictive modeling. In the previously discussed study by Yang et al. [110], selected ABVS radiomic and breath metabolomic features were combined with clinical variables and analyzed using an ensemble of random forest, logistic regression, and XGBoost classifiers. Early fusion is straightforward to implement and facilitates assessment of feature contributions, but differences in scale, dimensionality, and redundancy can cause modality imbalance and overfitting in small paired cohorts. Appropriate normalization and feature selection are therefore important to improve comparability, reduce redundancy, and balance feature contributions across modalities [116].

Intermediate-level fusion integrates learned modality-specific or shared representations before prediction. Tao et al. developed a multimodal deep-learning framework named GUARD for predicting sentinel lymph node metastasis in breast cancer [117]. The framework processes grayscale ultrasound, color Doppler, clinical report text, and serum metabolomics through separate encoders, aligns their representations through contrastive learning, and applies entropy-weighted feature fusion. However, the limited size of the paired ultrasound–metabolomics cohort increases the risk of overfitting and limits confidence in the model's generalizability. Latent-factor methods provide another form of intermediate-level integration. As discussed earlier, Xi et al. used subtensor factorization to identify associations between ultrasound radiomic features and genomic alterations [106]. In an MRI-based study, Guan et al. developed MVNMF, combining subspace learning and multiview regularization to select radiomic features informed by multiple genomic data types [113]. Its imaging-only prediction approach may also be evaluated in future ultrasound studies. Decision-level (late) fusion combines modality-specific predictions or diagnostic assessments through averaging, weighted voting, or a second-stage model. A related late-stage approach was used by Liu et al. [118], who combined cfDNA fragmentomics scores with independently assigned ultrasound and mammography BI-RADS categories in a joint machine-learning model. This study represents score-level integration of molecular predictions with imaging assessments rather than strict late fusion of separately trained ultrasound and molecular classifiers. Late fusion offers modularity and can accommodate missing modalities, but summarizing each modality as a prediction may obscure detailed cross-modal interactions; its performance therefore depends on the reliability and calibration of the constituent outputs, and each missing-modality configuration requires explicit validation [119]. Overall, the optimal fusion strategy depends on factors such as cohort size, feature dimensionality, and modality availability. Its suitability should be assessed through unbiased comparisons and validation in independent cohorts.

Challenges

The key bottlenecks in the future development of ultrasound multi-omics lie first in standardization. Differences in imaging systems, transducers, imaging parameters, ROI definitions, and feature extraction pipelines may lead to substantial intercenter variability in imaging phenotypes, particularly for emerging techniques such as SMI, SRUS, and viscoelasticity imaging. For these techniques, no globally unified acquisition protocol, ROI-drawing standard, or accepted diagnostic cut-off has been established, and parameters differ across scanner platforms and vendors, which limits multicenter reproducibility. Second, limited paired data remains a major challenge: high-quality ultrasound imaging, multi-omics profiling, and long-term clinical outcomes are often difficult to obtain comprehensively from the same patient, resulting in studies that are predominantly single-center or based on relatively small cohorts. Third, differences among modalities in spatial resolution, temporal scale, and patterns of missing data make simple feature concatenation insufficient to fully exploit their complementary information. Meanwhile, the interpretability of complex AI models and their performance in external validation remain inadequate

清華大學出版社 Tsinghua University Press | SciOpen

[104,120,121].

Therefore, future research should move beyond the pursuit of model performance alone toward the establishment of standardized, multicenter, longitudinal, and paired ultrasound-multi-omics cohorts, while fully leveraging the complementary phenotypes provided by B-mode ultrasound, CEUS, microvascular imaging, and elastography. The ultimate goal is not to replace pathological or molecular testing with ultrasound, but rather to establish a continuous mapping from "imaging phenotype-molecular mechanism-clinical decision-making", thereby further advancing advanced ultrasound from a noninvasive imaging tool into a noninvasive molecular phenotyping framework for precision diagnosis of breast cancer [104,105,109].

Conclusions

In summary, ultrasound imaging has advanced from conventional morphological imaging to multi-modality imaging enabling cross-scale characteristics of breast lesions to be captured with high efficiency. Such advances have enabled a vast number of examinations to be performed routinely, which has in turn driven a large body of research in computer-aided diagnosis. To date, AI-based analysis of ultrasound imaging has demonstrated promising results in supporting benign–malignant differentiation, molecular subtyping, lymph-node staging, and treatment-response prediction. The recent efforts to integrate ultrasound radiomics with molecular data may provide a route toward non-invasive molecular phenotyping; however, direct studies integrating ultrasound with multiple molecular omics layers remain scarce and largely proof-of-concept. Their potential role in individual-patient management remains unestablished and requires rigorous external validation and prospective assessment of clinical utility. Among the prerequisites for clinical translation, constructing large-scale, multicenter, longitudinal cohorts with paired imaging and multi-omics datasets remains the most critical bottleneck. Whilst, most of these cutting-edge techniques are still undergoing research investigation and have not yet met the standards for routine clinical use, as majority of clinical evidences largely came from retrospective or proof-of-concept studies, with few techniques validated prospectively across multiple centers. The emerging integration of ultrasound radiomics with multi-omics data offers a promising avenue for linking imaging phenotypes with genotypes, although this field is still developing albeit at an unprecedented speed.

Acknowledgements

Not applicable.

Funding

None

Authors' Contributions

VYW, GJT and DX contributed to the conceptualization and design of the review. ML, LTJ and MAB performed the investigation (literature search and data collection) and prepared the visualization (figures and tables). JYC and GX collected the multi-modality imaging data featured in this article. ML was responsible for writing the original draft. LTJ and GX revised the article. VYW, GJT and DX provided supervision throughout the preparation of this manuscript followed by final review and approval. All authors contributed to editorial changes in the manuscript. All authors read and approved the final manuscript. All authors have participated sufficiently in the work and agreed to be accountable for all aspects of the work.

Data Availability

All data generated or analyzed during this study are included in this article.

Declarations

Ethics approval and consent to participate

The use of anonymized retrospective patient images in this review was approved by the Ethics Committee of Zhejiang Cancer Hospital, Hangzhou, Zhejiang, China (Approval No. IRB-2026-158 [IIT]).

Consent for publication

Not applicable. All patient images included in this review were anonymized, and no personally identifiable information is presented.

Conflict of interest

The authors have no competing interests to declare that are relevant to the content of this article.

References

[1] Anderer S. Who releases global status report on cancer. Jama 2026;336:540.

[2] Kim J, Harper A, Mccormack V, Sung H, Houssami N, Morgan E, et al. Global patterns and trends in breast cancer incidence and mortality across 185 countries. Nat Med 2025;31:1154-1162.

[3] Giuliano A E, Edge S B, Hortobagyi G N. Eighth edition of the ajcc cancer staging manual: breast cancer. Ann Surg Oncol 2018;25:1783-1785.

[4] Guo L, Kong D, Liu J, Zhan L, Luo L, Zheng W, et al. Breast cancer heterogeneity and its implication in personalized precision therapy. Exp Hematol Oncol 2023;12:3.

[5] Weinstein S P, Slanetz P J, Lewin A A, Battaglia T, Chagpar A B, Dayaratna S, et al. Acr appropriateness criteria® supplemental breast cancer screening based on breast density. J Am Coll Radiol 2021;18:S456-s473.

[6] Aristokli N, Polycarpou I, Themistocleous S C, Sophocleous D, Mamais I. Comparison of the diagnostic performance of magnetic resonance imaging (mri), ultrasound and mammography for detec-

tion of breast cancer based on tumor type, breast density and patient's history: a review. Radiography (Lond) 2022;28:848-856.
[7] Evans A, Trimboli R M, Athanasiou A, Balleyguier C, Baltzer P A, Bick U, et al. Breast ultrasound: recommendations for information to women and referring physicians by the european society of breast imaging. Insights Imaging 2018;9:449-461.
[8] Llinas-Bertran A, Butjosa-Espín M, Barberi V, Seoane J A. Multimodal data integration in early-stage breast cancer. Breast 2025;80:103892.
[9] Kaplan S S. Clinical utility of bilateral whole-breast us in the evaluation of women with dense breast tissue. Radiology 2001;221:641-649.
[10] Jacobson J A, Middleton W D, Allison S J, Dahiya N, Lee K S, Levine B D, et al. Ultrasonography of superficial soft-tissue masses: society of radiologists in ultrasound consensus conference statement. Radiology 2022;304:18-30.
[11] Song H, Shu R, Uematsu T, Moon W K. Bi-rads v2025 for breast ultrasound: key updates and asian perspectives. Ultrasonography 2026;45:311-324.
[12] Stanzani D, Chala L F, Barros N, Cerri G G, Chammas M C. Can doppler or contrast-enhanced ultrasound analysis add diagnostically important information about the nature of breast lesions? Clinics (Sao Paulo) 2014;69:87-92.
[13] Watanabe T, Yamaguchi T, Okuno T, Konno S, Takaki R, Sato M, et al. Utility of b-mode, color doppler and elastography in the diagnosis of breast cancer: results of the cd-confirm multicenter study of 1351 breast solid masses. Ultrasound Med Biol 2021;47:3111-3121.
[14] Park A Y, Seo B K, Han M R. Breast ultrasound microvascular imaging and radiogenomics. Korean J Radiol 2021;22:677-687.
[15] Zhu J Y, He H L, Jiang X C, Bao H W, Chen F. Multimodal ultrasound features of breast cancers: correlation with molecular subtypes. BMC Med Imaging 2023;23:57.
[16] Li M, Li Q, Yin Q, Wang Y, Shang J M, Wang L H. Evaluation of color doppler ultrasound combined with plasma mir-21 and mir-27a in the diagnosis of breast cancer. Clin Transl Oncol 2021;23:709-717.
[17] Mehdikhani B, Benam M, Moradkhani A, Roostaee A, Bahman S S, Barmayoon P, et al. Evaluation of diagnostic value of doppler ultrasound in the diagnosis of malignant breast masses. Eur J Transl Myol 2024;34:12372.
[18] Keshavarz E, Karimi M A, Valian N, Kalantari M, Valian K. Diagnostic value of spectral doppler ultrasound in detecting breast malignancies: an original article. Int J Cancer Manag 2018;11:e8200.
[19] Zhang Q, Liang X, Zhang Y, Nie H, Chen Z. A review of contrast-enhanced ultrasound using sonovue® and sonazoid™ in non-hepatic organs. Eur J Radiol 2023;167:111060.
[20] Janu E, Krikavova L, Little J, Dvorak K, Brancikova D, Jandakova E, et al. Prospective evaluation of contrast-enhanced ultrasound of breast bi-rads 3-5 lesions. BMC Med Imaging 2020;20:66.
[21] Park A Y, Kwon M, Woo O H, Cho K R, Park E K, Cha S H, et al. A prospective study on the value of ultrasound microflow assessment to distinguish malignant from benign solid breast masses: association between ultrasound parameters and histologic microvessel densities. Korean J Radiol 2019;20:759-772.
[22] Chen C, Turco S, Kapetas P, Mann R, Wijkstra H, De Korte C, et al. Spatiotemporal analysis of contrast-enhanced ultrasound for differentiating between malignant and benign breast lesions. Eur Radiol 2024;34:4764-4773.
[23] Wang B, Yang D, Zhang X, Gong X, Xu T, Han J, et al. The diagnostic value of contrast-enhanced ultrasonography in breast ductal abnormalities. Cancer Imaging 2023;23:25.
[24] Li J K, Jin Z Y, Xu Y J, Fu N Q, Jiang Y, Li S Y, et al. Contrast-enhanced ultrasound to predict malignant upgrading of atypical ductal hyperplasia. Breast Cancer Res 2024;26:27.
[25] Zhang X, Cheng F, Song X, Wang P, Tian S, Zhao X, et al. Superb microvascular imaging for evaluation of microvascularity in breast nodules compared with conventional doppler imaging. Quant Imaging Med Surg 2023;13:7029-7040.
[26] Zhou F, Lin W, Yao J, Lu X, Yu L. Enhanced differentiation of breast lesions through integration of microvascular flow imaging and machine learning algorithms. Front Oncol 2026;16:1827050.
[27] Lee E J, Chang Y W, Oh E, Hwang J, Kim H J, Hong S S. Reproducibility and diagnostic performance of the vascular index of superb microvascular imaging in real-time breast ultrasonography for evaluating breast masses. Ultrasonography 2021;40:398-406.
[28] Lee E J, Chang Y W. Prediction of complete response after neoadjuvant chemotherapy for invasive breast cancers: the utility of shear wave elastography and superb microvascular imaging in pretreatment breast ultrasound. Eur J Radiol 2024;175:111432.
[29] Cai S, Wang H, Zhang X, Zhang L, Zhu Q, Sun Q, et al. Superb microvascular imaging technology can improve the diagnostic efficiency of the bi-rads system. Front Oncol 2021;11:634752.
[30] Zuo Y, Zhan Y, Zhou J, Xia H, Li T, Zhou F, et al. Prediction of pathological complete response to neoadjuvant chemotherapy for invasive breast cancers based on longitudinal ultrasound and superb microvascular imaging: a single-center retrospective study. PeerJ 2025;13:e20171.
[31] Zhang X Y, Cai S M, Zhang L, Zhu Q L, Sun Q, Jiang Y X, et al. Association between vascular index measured via superb microvascular imaging and molecular subtype of breast cancer. Front Oncol 2022;12:861151.
[32] Zhao G, Kong D, Xu X, Hu S, Li Z, Tian J. Deep learning-based classification of breast lesions using dynamic ultrasound video. Eur J Radiol 2023;165:110885.
[33] Dencks S, Lowerison M, Hansen-Shearer J, Shin Y, Schmitz G, Song P, et al. Super-resolution ultrasound: from data acquisition and motion correction to localization, tracking, and evaluation. IEEE Trans Ultrason Ferroelectr Freq Control 2025;72:408-426.
[34] Xia S, Zheng Y, Hua Q, Wen J, Luo X, Yan J, et al. Super-resolution ultrasound and microvasculomics: a consensus statement. Eur Radiol 2024;34:7503-7513.
[35] Liu F, Xia S, Hua Q, Yuan C, Zheng Y, Tao R, et al. Evaluation of tibial nerve microcirculation in diabetes mellitus at superresolution us. Radiology 2026;318:e250347.
[36] Opacic T, Dencks S, Theek B, Piepenbrock M, Ackermann D, Rix A, et al. Motion model ultrasound localization microscopy for preclinical and clinical multiparametric tumor characterization. Nat Commun 2018;9:1527.
[37] Hou X, Li Z, Liu Y, Gao J, Song T. Diagnostic value of super-resolution ultrasound imaging in differentiating benign and malignant bi-rads-4 breast lesions. Front Oncol 2025;15:1662492.
[38] Hua Q, Xia S, Yuan C, Li Y, Zheng Y, Tao R, et al. The super resolution ultrasound in visualizing interstitial-lymphatic network in breast tumors: a clinical pilot application. Acad Radiol 2026;33:2899-2910.
[39] Li J, Wei C, Ying T, Liu Y, Wang R, Li M, et al. Differentiation of benign and malignant breast lesions by ultrasound localization microscopy. Insights Imaging 2025;16:128.
[40] Xia S, Hua Q, Song Y, Yuan C, Zheng Y, Tao R, et al. Super-resolution ultrasound imaging of intranodal lymphatic sinuses for pre-

dicting sentinel lymph node metastasis in breast cancer: a preliminary study. Eur Radiol 2025;35:6079-6088.
[41] Zhang M, Zhang B. Extracellular matrix stiffness: mechanisms in tumor progression and therapeutic potential in cancer. Exp Hematol Oncol 2025;14:54.
[42] Kanagaraju V, Dhivya B, Devanand B, Maheswaran V. Utility of ultrasound strain elastography to differentiate benign from malignant lesions of the breast. J Med Ultrasound 2021;29:89-93.
[43] Barr R G, Nakashima K, Amy D, Cosgrove D, Farrokh A, Schafer F, et al. Wfumb guidelines and recommendations for clinical use of ultrasound elastography: part 2: breast. Ultrasound Med Biol 2015;41:1148-1160.
[44] Xu J, Zhang L, Wen W, He Y, Wei T, Zheng Y, et al. Evaluation of standard breast ultrasonography by adding two-dimensional and three-dimensional shear wave elastography: a prospective, multicenter trial. Eur Radiol 2024;34:945-956.
[45] Zhao Q Y, Zhao B, Wu G. Predictive value of shear wave elastography and molecular subtypes for postoperative efficacy in patients with early breast cancer. Ann Med 2025;57:2544879.
[46] Huang J X, Lin S Y, Ou Y, Shi C G, Zhong Y, Wei M J, et al. Combining conventional ultrasound and sonoelastography to predict axillary status after neoadjuvant chemotherapy for breast cancer. Eur Radiol 2022;32:5986-5996.
[47] Tekcan Sanli D E, Yildirim D, Kandemirli S G, Sanli A N, Aribal E. Evaluation of multiparametric shear wave elastography indices in malignant and benign breast lesions. Acad Radiol 2022;29(Suppl 1):S50-s61.
[48] Barr R G, Engel A, Kim S, Tran P, De Silvestri A. Improved breast 2d swe algorithm to eliminate false-negative cases. Invest Radiol 2023;58:703-709.
[49] Osika M, Kijanka P. Ultrasound shear wave propagation modeling in general tissue-like viscoelastic materials. Ultrasound Med Biol 2024;50:627-638.
[50] Kumar V, Denis M, Gregory A, Bayat M, Mehrmohammadi M, Fazzio R, et al. Viscoelastic parameters as discriminators of breast masses: initial human study results. PLoS One 2018;13:e0205717.
[51] Hossain M M, Gallippi C M. Viscoelastic response ultrasound derived relative elasticity and relative viscosity reflect true elasticity and viscosity: in silico and experimental demonstration. IEEE Trans Ultrason Ferroelectr Freq Control 2020;67:1102-1117.
[52] Woo E, Lee J Y, Seo B K, Bae M S, Park E K, Choi H, et al. Diagnostic performance of shear-wave dispersion imaging and shear-wave elastography for differentiating benign and malignant breast masses. Eur Radiol 2026;36:3378-3391.
[53] Jia W, Xia S, Jia X, Tang B, Cheng S, Nie M, et al. Ultrasound viscosity imaging in breast lesions: a multicenter prospective study. Acad Radiol 2024;31:3499-3510.
[54] Bae M S, Kim H Y, Oh H, Seo B K. Clinical applications of shear wave dispersion imaging for breast lesions: a pictorial essay. Ultrasonography 2023;42:589-599.
[55] Yang Z, Li X. A combined model of ultrasound viscoelasticity and inflammatory indices for differentiating benign and malignant breast lesions. BMC Med Imaging 2026;26:96.
[56] Tao J, Niu Z, Zhou M, Zhao J, Xiao M, Zhu Q. Viscoelastic mechanical properties assessed by ultrasound correlates with tumor proliferation in invasive ductal breast cancer: a preliminary study. Ultrasound Med Biol 2026;52:984-990.
[57] Xu J, Shi J, Huang Y, Chen C, Xiang G, Zheng W, et al. Diagnostic value of ultrasound peritumoral viscoelasticity parameters in breast cancer: enhancing bi-rads classification performance. BMC Med Imaging 2026;26:95.
[58] Xiao X Y, Chen X, Guan X F, Wu H, Qin W, Luo B M. Superb microvascular imaging in diagnosis of breast lesions: a comparative study with contrast-enhanced ultrasonographic microvascular imaging. Br J Radiol 2016;89:20160546.
[59] Luo J, Li T, Liu Y. Diagnostic value of the vascular index measured by superb microvascular imaging for evaluating breast tumors: a meta-analysis. Med Ultrason 2023;25:415-422.
[60] Lee E J, Chang Y W. Combination of quantitative parameters of shear wave elastography and superb microvascular imaging to evaluate breast masses. Korean J Radiol 2020;21:1045-1054.
[61] Kurt S A, Kayadibi Y, Saracoglu M S, Ozturk T, Korkmazer B, Cerit M, et al. Prediction of molecular subtypes using superb microvascular imaging and shear wave elastography in invasive breast carcinomas. Acad Radiol 2023;30:14-21.
[62] Cui X W, Li K N, Yi A J, Wang B, Wei Q, Wu G G, et al. Ultrasound elastography. Endosc Ultrasound 2022;11:252-274.
[63] Golatta M, Pfob A, Büsch C, Bruckner T, Alwafai Z, Balleyguier C, et al. The potential of combined shear wave and strain elastography to reduce unnecessary biopsies in breast cancer diagnostics - an international, multicentre trial. Eur J Cancer 2022;161:1-9.
[64] Li J, Sun B, Li Y, Li S, Wang J, Zhu Y, et al. Correlation analysis between shear-wave elastography and pathological profiles in breast cancer. Breast Cancer Res Treat 2023;197:269-276.
[65] Bai L, You C, Zhou J, Xie L, Zhu X, Chang C, et al. Quantitative analysis of shear wave elastography and us-guided diffuse optical tomography for evaluating biological characteristics of breast cancer. Acad Radiol 2024;31:3489-3498.
[66] Liu H C, Lee H K, Urban M W, Zhou Q, Kijanka P. Acoustic radiation force-induced longitudinal shear wave for ultrasound-based viscoelastic evaluation. Ultrasonics 2024;142:107389.
[67] Liu Z, Liu W, Chen Q, Hu Y, Li Y, Zheng X, et al. Real-time non-destructive viscosity measurement of soft tissue based on viscoelastic response optical coherence elastography. Materials (Basel) 2023;16:6019.
[68] Zhang J, He Q, Xiao Y, Zheng H, Wang C, Luo J. Ultrasound image reconstruction from plane wave radio-frequency data by self-supervised deep neural network. Med Image Anal 2021;70:102018.
[69] Ouyang Y, Tsui P H, Wu S, Wu W, Zhou Z. Classification of benign and malignant breast tumors using h-scan ultrasound imaging. Diagnostics (Basel) 2019;9:182.
[70] Wang Q, Jia X, Luo T, Yu J, Xia S. Deep learning algorithm using bispectrum analysis energy feature maps based on ultrasound radiofrequency signals to detect breast cancer. Front Oncol 2023;13:1272427.
[71] Baek J, O'connell A M, Parker K J. Improving breast cancer diagnosis by incorporating raw ultrasound parameters into machine learning. Mach Learn Sci Technol 2022;3:045013.
[72] Xie Z, Sun Q, Han J, Sun P, Hu X, Ji N, et al. Spectral analysis enhanced net (sae-net) to classify breast lesions with bi-rads category 4 or higher. Ultrasonics 2024;143:107406.
[73] Sheibani-Asl N, Osapoetra L O, Czarnota G J, Sadeghi-Naini A. Ai-enabled rf data synthesis for breast ultrasound: efficacy in quantitative ultrasound tissue characterization. Sci Rep 2026;16:12544.
[74] Wei Q, Yan Y J, Wu G G, Ye X R, Jiang F, Liu J, et al. The diagnostic performance of ultrasound computer-aided diagnosis system for distinguishing breast masses: a prospective multicenter study. Eur Radiol 2022;32:4046-4055.
[75] Gu Y, Xu W, Liu T, An X, Tian J, Ran H, et al. Ultrasound-based deep learning in the establishment of a breast lesion risk stratification system: a multicenter study. Eur Radiol 2023;33:2954-2964.
[76] Shen Y, Shamout F E, Oliver J R, Witowski J, Kannan K, Park J, et

al. Artificial intelligence system reduces false-positive findings in the interpretation of breast ultrasound exams. Nat Commun 2021;12:5645.

[77] Mango V L, Sun M, Wynn R T, Ha R. Should we ignore, follow, or biopsy? impact of artificial intelligence decision support on breast ultrasound lesion assessment. AJR Am J Roentgenol 2020;214:1445-1452.

[78] Lai Y C, Chen H H, Hsu J F, Hong Y J, Chiu T T, Chiou H J. Evaluation of physician performance using a concurrent-read artificial intelligence system to support breast ultrasound interpretation. Breast 2022;65:124-135.

[79] Chen H, Li Y, Zhang J, Yang L, Sun Y, Chen Y, et al. An alignment and imputation network (ainet) for breast cancer diagnosis with multimodal multi-view ultrasound images. IEEE Trans Med Imaging 2026;45:1383-1394.

[80] Cai L, Pfob A, Barr R G, Duda V, Alwafai Z, Balleyguier C, et al. Deep learning model for breast shear wave elastography to improve breast cancer diagnosis (inspired 006): An international, multicenter analysis. J Clin Oncol 2025;43:3482-3493.

[81] Qian X, Pei J, Han C, Liang Z, Zhang G, Chen N, et al. A multimodal machine learning model for the stratification of breast cancer risk. Nat Biomed Eng 2025;9:356-370.

[82] Jiang M, Zhang D, Tang S C, Luo X M, Chuan Z R, Lv W Z, et al. Deep learning with convolutional neural network in the assessment of breast cancer molecular subtypes based on us images: a multicenter retrospective study. Eur Radiol 2021;31:3673-3682.

[83] Zhou L Q, Wu X L, Huang S Y, Wu G G, Ye H R, Wei Q, et al. Lymph node metastasis prediction from primary breast cancer us images using deep learning. Radiology 2020;294:19-28.

[84] Nicholson W K, Silverstein M, Wong J B, Barry M J, Chelmow D, Coker T R, et al. Screening for breast cancer: us preventive services task force recommendation statement. Jama 2024;331:1918-1930.

[85] Marcon M, Fuchsjäger M H, Clauser P, Mann R M. Esr essentials: Screening for breast cancer - general recommendations by eusobi. Eur Radiol 2024;34:6348-6357.

[86] Ding R, Xiao Y, Mo M, Zheng Y, Jiang Y Z, Shao Z M. Breast cancer screening and early diagnosis in chinese women. Cancer Biol Med 2022;19:450-467.

[87] Wang J, Zheng S, Ding L, Liang X, Wang Y, Greuter M J W, et al. Is ultrasound an accurate alternative for mammography in breast cancer screening in an asian population? a meta-analysis. Diagnostics (Basel) 2020;10:985.

[88] Uematsu T, Izumori A, Moon W K. Overcoming the limitations of screening mammography in japan and korea: a paradigm shift to personalized breast cancer screening based on ultrasonography. Ultrasonography 2023;42:508-517.

[89] Payne N R, Hickman S E, Black R, Priest A N, Hudson S, Gilbert F J. Breast density effect on the sensitivity of digital screening mammography in a uk cohort. Eur Radiol 2025;35:177-187.

[90] Harada-Shoji N, Suzuki A, Ishida T, Zheng Y F, Narikawa-Shiono Y, Sato-Tadano A, et al. Evaluation of adjunctive ultrasonography for breast cancer detection among women aged 40-49 years with varying breast density undergoing screening mammography: a secondary analysis of a randomized clinical trial. JAMA Netw Open 2021;4:e2121505.

[91] Güldoğan N, Ulus S, Kovan Ö, Aksan A, Tokmakçıoğlu K, Camgöz Akdağ H, et al. Evaluating efficiency of time use and operational costs in a breast clinic workflow: a comparative analysis between automated breast ultrasound and handheld ultrasound. Eur J Breast Health 2023;19:311-317.

[92] Klein Wolterink F, Ab Mumin N, Appelman L, Derks-Rekers M, Imhof-Tas M, Lardenoije S, et al. Diagnostic performance of 3d automated breast ultrasound (3d-abus) in a clinical screening setting-a retrospective study. Eur Radiol 2024;34:5451-5460.

[93] Gatta G, Cappabianca S, La Forgia D, Massafra R, Fanizzi A, Cuccurullo V, et al. Second-generation 3d automated breast ultrasonography (prone abus) for dense breast cancer screening integrated to mammography: effectiveness, performance and detection rates. J Pers Med 2021;11:875.

[94] Park C K S, Trumpour T, Aziz A, Bax J S, Tessier D, Gardi L, et al. Cost-effective, portable, patient-dedicated three-dimensional automated breast ultrasound for point-of-care breast cancer screening. Sci Rep 2023;13:14390.

[95] Shen Y, He J, Liu M, Hu J, Wan Y, Zhang T, et al. Diagnostic value of contrast-enhanced ultrasound and shear-wave elastography for small breast nodules. PeerJ 2024;12:e17677.

[96] Li C, Wu M, Haiqing H. The application of multimodal ultrasound examination in the differential diagnosis of benign and malignant breast lesions of bi-rads category 4. Front Med (Lausanne) 2025;12:1596100.

[97] Wang X, He Y, Wang L. Diagnostic value of shear wave elastography combined with super microvascular imaging for bi-rads 3-5 nodules. Front Oncol 2023;13:1192630.

[98] Yang Z, Lyu Y, Yang Y, Xu C, Zhang K, Yang X, et al. Application of multimodal ultrasound combined with bi-rads in classification and diagnosis of non-mass breast lesions. J Clin Ultrasound 2026;54:609-617.

[99] Niu Z, Gao Y, Xiao M, Mao F, Zhou Y, Zhu Q, et al. Contrast-enhanced lymphatic us can improve the preoperative diagnostic performance for sentinel lymph nodes in early breast cancer. Eur Radiol 2023;33:1593-1602.

[100] Zhuang L, Ming X, Liu J, Jia C, Jin Y, Wang J, et al. Comparison of lymphatic contrast-enhanced ultrasound and intravenous contrast-enhanced ultrasound in the preoperative diagnosis of axillary sentinel lymph node metastasis in patients with breast cancer. Br J Radiol 2022;95:20210897.

[101] Li S Y, Li Y M, Fang Y Q, Jin Z Y, Li J K, Zou X M, et al. Contrast-enhanced ultrasound radiomics model for predicting axillary lymph node metastasis and prognosis in breast cancer: a multicenter study. BMC Cancer 2025;25:1315.

[102] Huang D, Shi Y, Cao W, Feng L, Luo Y, Zhao X, et al. Exempting axillary staging surgery in breast cancer using multimodal ultrasound imaging and radiomics of sentinel lymph nodes. EClinicalMedicine 2026;92:103782.

[103] Xu S, Wang Q, Hong Z. The correlation between multi-mode ultrasonographic features of breast cancer and axillary lymph node metastasis. Front Oncol 2024;14:1433872.

[104] Jiang B, Wu Y, Chen X, Jian C, Wang W. Artificial intelligence and multi-omics convergence in breast cancer: revolutionizing diagnosis, prognostication, and precision oncology. Crit Rev Oncol Hematol 2026;220:105160.

[105] Qi Y J, Su G H, You C, Zhang X, Xiao Y, Jiang Y Z, et al. Radiomics in breast cancer: current advances and future directions. Cell Rep Med 2024;5:101719.

[106] Xi J, Sun D, Chang C, Zhou S, Huang Q. An omics-to-omics joint knowledge association subtensor model for radiogenomics cross-modal modules from genomics and ultrasonic images of breast cancers. Comput Biol Med 2023;155:106672.

[107] Peng X, Zhou X, Feng X, Fang N, Dong X, Hong W, et al. Artificial intelligence for triple-negative breast cancer from imaging to multi-omics. Front Oncol 2026;16:1834128.

[108] Ran D, Li J, Zhao M, Du L, Zhang Y, Zhu J. Artificial intelligence integrates multi-omics data for precision stratification and drug resistance prediction in breast cancer. Front Oncol 2025;15:1612474.

[109] Wu X, Dai W. Beyond imaging: integrating radiomics, genomics, and multi-omics for precision breast cancer management. Cancers (Basel) 2025;17:3408.

[110] Yang Y, Long H, Feng Y, Tian S, Chen H, Zhou P. A multi-omics method for breast cancer diagnosis based on metabolites in exhaled breath, ultrasound imaging, and basic clinical information. Heliyon 2024;10:e32115.

[111] Jiang L, You C, Xiao Y, Wang H, Su G H, Xia B Q, et al. Radiogenomic analysis reveals tumor heterogeneity of triple-negative breast cancer. Cell Rep Med 2022;3:100694.

[112] Su G H, Xiao Y, You C, Zheng R C, Zhao S, Sun S Y, et al. Radiogenomic-based multiomic analysis reveals imaging intratumor heterogeneity phenotypes and therapeutic targets. Sci Adv 2023;9:eadf0837.

[113] Guan J, Fan M, Li L. Mvnmf: Multiview nonnegative matrix factorization for radio-multigenomic analysis in breast cancer prognosis. Med Image Anal 2025;103:103566.

[114] Huang S C, Pareek A, Seyyedi S, Banerjee I, Lungren M P. Fusion of medical imaging and electronic health records using deep learning: a systematic review and implementation guidelines. NPJ Digit Med 2020;3:136.

[115] Picard M, Scott-Boyer M P, Bodein A, Périn O, Droit A. Integration strategies of multi-omics data for machine learning analysis. Comput Struct Biotechnol J 2021;19:3735-3746.

[116] Chicco D, Cumbo F, Angione C. Ten quick tips for avoiding pitfalls in multi-omics data integration analyses. PLoS Comput Biol 2023;19:e1011224.

[117] Tao W, Jiang Q, Shan J, Yang Z, Zhang Y, Lu H, et al. A multimodal deep learning framework to predict breast cancer sentinel lymph node metastasis in ultrasound images with metabolomics interpretation. Current Genomics 2026.

[118] Liu J, Li Y, Tang W, Qian T, Dai L, Jia Z, et al. Cell-free DNA fragmentomics assay to discriminate the malignancy of breast nodules and evaluate treatment response. Genomics Proteomics Bioinformatics 2025;23:qzaf028.

[119] Cui C, Yang H, Wang Y, Zhao S, Asad Z, Coburn L A, et al. Deep multimodal fusion of image and non-image data in disease diagnosis and prognosis: a review. Prog Biomed Eng (Bristol) 2023;5.

[120] Omran M M, Emam M, Gamaleldin M, Abushady A M, Elattar M A, El-Hadidi M. Comparative analysis of statistical and deep learning-based multi-omics integration for breast cancer subtype classification. J Transl Med 2025;23:709.

[121] Tong L, Mitchel J, Chatlin K, Wang M D. Deep learning based feature-level integration of multi-omics data for breast cancer patients survival analysis. BMC Med Inform Decis Mak 2020;20:225.